

Investigation of submicron particles as emulsion stabilizers

Daniel Guilherme Henriques Vicente

Thesis to obtain the Master of Science Degree in

Chemical Engineering

Supervisor(s): Prof. Ana Clara Lopes Marques
Prof. António Correia Diogo

Examination Committee

Chairperson: Prof. Sebastião Manuel Tavares da Silva Alves
Supervisor(s): Prof. Ana Clara Lopes Marques
Members of the Committee: Maria Clara Henriques Baptista Gonçalves

February 2019

Acknowledgements

All the effort I put in this work would not be possible without a few people, which I think a thank you is needed.

I would like to thank my family for the patient and support for all those years, specially my sisters.

A sincere thank you for my supervisor Prof. Ana Clara Lopes, for all the support during this thesis, providing me with advice and for the opportunity to work under new subject that i find promising.

Finally, to the people of lab -2, specially Mario Vale, Monica Loureiro and David Duarte for all the help in the lab and for the way I was received. It was great environment for me to conduct this work.

Table of contents

Acknowledgements	ii
Abstract.....	i
Resumo	ii
Figure index	iii
Table index	v
Abbreviation list	vi
Symbol List	vii
1. Theoretical introduction	1
1.1. Motivation	1
1.2. Emulsions	1
1.2.1. Stability Studies	7
1.2.2. Pickering Emulsion	8
1.3. Hybrid porous microspheres.....	9
1.4. Silica submicron particles by a modified Stöber method.....	11
1.5. Hydrophobic treatment	12
1.6. Objective and work strategy	13
2.1. Materials	15
2.2. Methods.....	17
2.2.1. Synthesis of porous silica hybrid microspheres by microemulsion combined with sol-gel process	17
2.2.2. Characterization of the porous silica hybrid microspheres.....	19
2.2.3. Synthesis of silica submicron particles by a modified Stöber method.....	20
.....	22
2.2.4. Characterization of silica submicron particles	22
2.2.5. Characterization of silica commercial particles	22
2.2.6. Hydrophobic treatment	22
2.2.7. Characterization of silica hydrophobic particles	23
2.2.8. Emulsion stability studies	23
3. Results and discussion.....	25
Part I - Silica hybrid porous microspheres.....	25
3.1. Synthesis of silica hybrid porous microspheres.	25
Part II - Silica submicron particles for emulsion stability.	30
3.2. Synthesis of silica submicron particles by a modified Stöber method.....	30
3.3. Silica commercial particles	33
3.4. Hydrophobic treatment	35
PART III – Emulsion stability	37
3.5. Emulsion stability studies	37
3.5.1. Effect of the surfactant.....	37
3.5.2. Effect of the particles	46
PART IV – Evaluating the stability results on the synthesis process	59
3.6. New synthesis.....	59
4. Conclusions.....	62
5. Future work	63
6. References.....	64

Declaration

I declare that this document is an original work of my own authorship and that it fulfills all the requirements of the Code of Conduct and Good Practices of the Universidade de Lisboa.

Abstract

Porous microspheres of silica or hybrid composition play an important role in numerous applications. One of them is as microscaffolds, which have specific chemicals grafted, immobilized or stored, for a targeted effect either by contact or by controlled release. These microscaffolds are possible to be prepared by microemulsion techniques combined with the sol-gel method. The stability of the emulsions is a key factor for those microscaffolds quality.

The first stage of this work regarded the optimization of the porous microspheres synthesis procedure. Several studies were performed, evaluating the effect on the resulting microspheres of the surfactant concentration, the emulsification speed, and the mechanical stirring speed. The critical parameters were then chosen taking into account the particle morphology and the size distribution.

The second stage of this work regarded the synthesis of silica submicron particles, developed as emulsion stabilizing agents, their hydrophobization treatment using hexadecyltrimethoxysilane to make them more suitable for water-in-oil emulsions and their comparison with commercial available particles.

The submicron particles were tested as emulsion stabilizing agents, at different concentrations, and their effect was compared with that of typical surfactants, namely SPAN 80, currently used in the synthesis of the microspheres, and Pluronic P123, on a water-in-oil emulsion using decahydronaphthalene as oil phase. The emulsion stability was evaluated by visual and microscopy observation, and the emulsion volume fraction was assessed along the time, as well as the evolution of the emulsion droplets size and their distribution. Small silica particles of 200 nm in diameter with a hydrophobization surface treatment at a concentration in the range of ca. 2 to 5 wt% (relative to the organic phase) were the ones exhibiting better performance as emulsion (W/O) stabilizers.

Key-words: Pickering emulsions, emulsion stability testing, silica particle synthesis, hydrophobic treatment.

Resumo

As microesferas porosas de sílica ou de composição híbrida desempenham um papel importante em inúmeras aplicações. Uma delas é como *microscaffolds*, que contêm químicos específicos ligados covalentemente, imobilizados ou armazenados, para aplicação localizada por contacto ou por libertação controlada. Estes *microscaffolds* podem ser preparados por técnicas de microemulsão combinadas com o método sol-gel. A estabilidade dessas emulsões é um parâmetro chave para a qualidade dos *microscaffolds* resultantes.

O objetivo desta tese é o desenvolvimento de partículas submicrométricas para uso como estabilizadores de emulsões água-em-óleo e potencialmente substituir o uso de tensoativos.

A primeira fase deste trabalho visou a otimização do processo de síntese das microesferas porosas. Vários estudos foram realizados para avaliar o efeito da concentração de tensoativo, da velocidade de emulsificação e a velocidade de agitação mecânica nas microesferas resultantes. Os parâmetros críticos foram escolhidos com base na morfologia e distribuição de tamanho.

A segunda fase deste trabalho envolveu a síntese de partículas submicrométricas, para aplicação como agentes de estabilização de emulsões, usando hexadeciltrimetoxisilano para o seu tratamento de hidrofobização de forma a tornar as partículas mais apropriadas para uso em emulsões água-em-óleo e a sua comparação com partículas disponíveis comercialmente.

As partículas submicrométricas foram testadas como agentes estabilizadores de emulsões a diferentes concentrações, e o seu efeito foi comparado com o de dois tensoativos comuns, nomeadamente o SPAN 80, usado correntemente na síntese das microesferas e o Pluronic P123, numa emulsão água-em-óleo usando deca-hidronaftaleno como fase óleo. A estabilidade da emulsão foi avaliada por observação visual e ao microscópio, e a fração de volume de emulsão foi avaliada ao longo do tempo, assim como a evolução do tamanho e distribuição das gotículas. As partículas que revelaram melhor desempenho na estabilização de emulsões do tipo água-em-óleo, foram partículas de sílica de diâmetro 200 nm com tratamento superficial hidrófobo, a uma concentração de ca 2 a 5 (m/m)% relativamente à fase orgânica.

Palavras-chave: Emulsões de Pickering, testes de estabilidade de emulsões, síntese de partículas de sílica, tratamento hidrófobo.

Figure index

Figure 1 – Pictorial representation of the different types of emulsions	2
Figure 2 – Pictorial representation of the emulsions instability mechanisms	4
Figure 3 - Schematic representation of the distribution of a surfactant in the water/oil interface	5
Figure 4 – Molecular structure of SPAN 80	6
Figure 5 - Schematic of a solid particle in the water-oil interface	8
Figure 6 - Schematic representation of the sol-gel process	10
Figure 7 – Molecular structure of TEOS and GPTMS	11
Figure 8 - Schematic representation of the Stöber process using TEOS as Si precursor	12
Figure 9 – Schematic representation of the hydrophobic treatment process	13
Figure 10 - Schematic representation of the pre-hydrolysis step	19
Figure 11 - Schematic representation of the emulsification step	19
Figure 12 - Schematic representation of the synthesis, filtration and drying steps	19
Figure 13 - Schematic representation of the synthesis of silica submicron particles	22
Figure 14 - SEM photomicrographs of SD23	25
Figure 15 - SEM photomicrograph of SD24	26
Figure 16 - SEM photomicrographs of SD25 and SD26	26
Figure 17 - SEM photomicrograph of SD27	27
Figure 18 - SEM photomicrographs of SD29 and of SD32	27
Figure 19 - SEM photomicrograph of SD26	27
Figure 20 - SEM photomicrograph of SD30	28
Figure 21 - SEM photomicrograph of SD31	29
Figure 22 - FTIR spectrum of SD23	29
Figure 23 - SEM photomicrographs of SD28 and SD36	30
Figure 24 - SEM photomicrographs of SD39, SD40 and SD42	31
Figure 25 – SEM photomicrograph of SD44	31
Figure 26 - SEM photomicrograph of SD34	31
Figure 27 – SEM photomicrographs of SD44 (100% KCl), SD48 (92% KCl) and SD46 (84% KCl)	32
Figure 28 - SEM photomicrograph of SD36	32
Figure 29 - FTIR spectrum of SD28 particles	33
Figure 30 - SEM photomicrographs of N2N	34
Figure 31 - SEM photomicrograph of N3N1	34
Figure 32 - SEM photomicrograph of N3N3	34
Figure 33 - SEM photomicrograph of N6N3	35
Figure 34 - SEM photomicrographs of SD36H	35
Figure 35 - SEM photomicrographs of N2NH	36
Figure 36 – SEM photomicrographs of SD36 and SD36H	36
Figure 37 - SEM photomicrographs of N2N and N2NH	36
Figure 38 – FTIR spectrums of the submicron particles	37
Figure 39 – Separation of oil and water phases from an emulsion	38
Figure 40 – Evolution of the W/O emulsion using 2g of SPAN 80	39
Figure 41 - Optical micrographs of emulsion using 2g of SPAN 80	39
Figure 42 - Evolution of the emulsion using 4g of SPAN 80 from 0 hours to 8 days.	39
Figure 43 - Optical micrographs of emulsion using 4g of SPAN at 0 hours and at 2 weeks	40
Figure 44 - Evolution of the emulsion using 6g of SPAN 80 from 0 hours to 8 days	40
Figure 45 – Optical micrographs of emulsion using 6g at 0 hours and at 2 weeks	40
Figure 46 - Evolution of the emulsion using 8g of SPAN 80 from 0 hours to 8 days	40
Figure 47 - Optical micrographs of emulsion using 8g at 0 hours and at 2 weeks	41
Figure 48 – Plot of the evolution of the emulsion with SPAN 80.	41
Figure 49 - Evolution of the emulsion using 2g of Pluronic P123 from 0 hours to 8 days	42
Figure 50 - Optical micrographs of emulsion using 2g of Pluronic P123 at 0h and at 2 weeks	42
Figure 51 - Evolution of the emulsion using 4g of Pluronic P123 from 0 hours to 8 days	42
Figure 52 - Optical micrographs of emulsion using 4g of Pluronic P123 at 0 hours and at 2 weeks	43
Figure 53 - Evolution of the emulsion using 6g of Pluronic P123 from 0 hours to 8 days	43
Figure 54 - Optical micrographs of emulsion using 6g of Pluronic P123 0h and at 2 weeks	43
Figure 55 - Evolution of the emulsion using 8g of Pluronic P123 from 0 hours to 8 days	43
Figure 56 - Optical micrographs of emulsion using 8g of Pluronic at 0 hours and at 2 weeks	44

Figure 57 - Evolution of the emulsion using 10g of Pluronic P123 from 0 hours to 4 weeks	44
Figure 58 - Optical micrographs of emulsion using 10g of Pluronic P123 at 0 hours and at 2 weeks	44
Figure 59 - Evolution of the emulsion using 12g of Pluronic P123 from 0 hours to 4 weeks	44
Figure 60 - Optical micrographs of emulsion using 12g of Pluronic P123 at 0 hours and at 2 weeks	45
Figure 61 - Plot of the evolution of the emulsion with Pluronic P123.	45
Figure 62 - Evolution of the emulsion using 0.2% of SD36 particles from 0 hours to 4 weeks.	46
Figure 63 - Optical micrographs of emulsion using 0.2% of SD36 particles at 0 hours	47
Figure 64 - Evolution of the emulsion using 2% of SD36 particles from 0 hours to 4 weeks.	47
Figure 65 - Optical micrographs of emulsion using 2% of SD36 particles at 0 hours, at 1 week and at 2 weeks	47
Figure 66 - Evolution of the emulsion using 0.2% of SD36H particles from 0 hours to 4 weeks	48
Figure 67 - Optical micrographs of emulsion using 0.2% of SD36H particles at 0 hours and after 4 weeks	48
Figure 68 - Plot with the evolution of emulsion using the particles	48
Figure 69 - Evolution of the emulsion using 0.2% of N3N1 particles from 0 hours to 4 weeks	49
Figure 70 - Optical micrograph of emulsion using 0.2% of N3N1 particles at 0 hours.	49
Figure 71 - Evolution of the emulsion using 2% of N3N1 particles from 0 hours to 2 weeks	50
Figure 72 - Optical micrograph of emulsion using 2% of N3N1 particles at 0 hours	50
Figure 73 - Evolution of the emulsion using 5.3% of N3N1 particles from 0 hours to 4 weeks	50
Figure 74 - Optical micrograph of emulsion using 5.3% of N3N1 particles at 0 hours	50
Figure 75 - Evolution of the emulsion using 0.2% of N3N3 particles from 0 hours to 4 weeks	51
Figure 76 - Optical micrograph of emulsion using 0.2% of N3N3 particles at 0 hours.	51
Figure 77 - Evolution of the emulsion using 2% of N3N3 particles from 0 hours to 2 weeks	51
Figure 78 - Optical micrograph of emulsion using 2% of N3N3 particles from 0 hours particles	51
Figure 79 - Evolution of the emulsion using 5.3% of N3N3 particles from 0 hours to 4 weeks	52
Figure 80 - Optical micrograph of emulsion using 5.3% of N3N3 particles at 0 hours	52
Figure 81 - Evolution of the emulsion using 0.2% of N6N3 particles from 0 hours to 4 weeks.	52
Figure 82 - Optical micrograph of emulsion using 0.2% of N6N3 particles at 0 hours	53
Figure 83 - Evolution of the emulsion using 2% of N6N3 particles from 0 hours to 4 weeks	53
Figure 84 - Optical micrographs of emulsion using 2% of N6N3 particles at 0 hours and at 2 weeks	53
Figure 85 - Evolution of the emulsion using 5.3% of N6N3 particles from 0 hours to 4 weeks	53
Figure 86 - Optical micrograph of emulsion using 5.3% of N6N3 particles at 0 hours	54
Figure 87 - Evolution of the emulsion using 2% of N2N particles from 0 hours to 5 days	54
Figure 88 - Optical micrographs of emulsion using 2% of N2N particles at 0 hours and 5 days.	54
Figure 89 - Evolution of the emulsion using 0.2% of N2NH particles from 0 hours to 5 days	55
Figure 90 - Optical micrographs of emulsion using 0.2% of N2NH particles at 0 hours and after 1 day	55
Figure 91 - Evolution of the emulsion using 2% of N2NH particles from 0 hours to 5 days	55
Figure 92 - Optical micrographs of emulsion using 2% of N2NH particles at 0 hours, 1 day, 2 days, 4 days and 5 days	56
Figure 93 - Evolution of the emulsion using 5.3% of N2NH particles from 0 hours to 5 days	56
Figure 94 - Optical micrographs of emulsion using 5.3% of N2NH particles at 0 hours and 5 days	56
Figure 95 - Plot with the evolution of emulsion with N2N and N2NH particles	57
Figure 96 - SEM photomicrographs of SD50 (10g Pluronic P123) and SD52 (8g Pluronic P123)	60
Figure 97 - SEM photomicrographs of SD53	60
Figure 98 - Optical micrographs of emulsion in the synthesis while using 2% of N2NH particles-	61

Table index

Table 1 – HLB values range and typical uses.	7
Table 2 – Compounds used and their suppliers.	15
Table 3 – Physical and chemical properties of the compounds employed.	16
Table 4 – Steps of temperature employed in the synthesis.	18
Table 5 – Sol-gel synthesis operational conditions and samples	18
Table 6 – Feeding profile of solution to the reactor	20
Table 7 - Stöber modified process samples	21
Table 8 - Surfactant test samples	23
Table 9 – Particle stability studies samples	24

Abbreviation list

O/W: oil-in-water
W/O: water-in-oil
W/O/W: water-in-oil.in-water
O/W/O: oil-in-water.in-oil
HLB: Hydrophilic-Lipophilic Balance
MS: microspheres
MC: microcapsules
JCP: Janus colloidal particles
TEOS: Tetraethyl orthosilicate
GPTMS: 3-Glycidyloxypropyl)trimethoxysilane
HDTMS: Hexadecyltrimethoxysilane
SPAN: SPAN 80
Pluronic: Pluronic P123
Dacalin: Decahydronaphthalene
TEOS: Xiameter OFS-6697 Silane
N3N1: HIPRESICA SS N3N 1 μm
N3N3: HIPRESICA TS N3N 3 μm
N6N3: HIPRESICA TS N6N 3 μm
N2N: HIPRESICA FQ N2N 0.2 μm
w/w%: weight by weight percentage
FTIR Fourier transformed infrared spectroscopy
SEM: Scanning electron microscopy

Symbol List

V_{stokes} – velocity of creaming/sedimentation
 g – acceleration of gravity
 r – radius of a droplet
 ρ – density
 η – viscosity of the liquid
 T – temperature
 K_b – Boltzmann constant
 D – diffusion coefficient
 ΔG – free energy
 γ - interfacial tension
 ΔA - total interfacial area of the disperse phase
 ΔP - interface pressure difference of the droplet
 θ - three-phase contact angle

1. Theoretical introduction

1.1. Motivation

Emulsions are used in various fields of work. Some of the applications are food industry, drug delivery and release, porous biomaterials to serve as tissue scaffolds, environment-responsive materials, catalysis, pharmaceuticals, energy industry, tissue engineering, separations, extracting and solid catalysts. However, in order to remain stable, they require the use of a stabilizer which most of the times is not safe for human or animal purposes. [1–3]. An alternative that can be used is to replace these stabilizers with solid particles.

The specific motivation of this work was to study a new emulsion stability strategy to be employed in the synthesis of porous microspheres of silica or hybrid composition which have been developed by A. Marques's group within the Technology Platform on Microencapsulation and Immobilization (<http://web.tecnico.ulisboa.pt/ana.marques/SiteTPMI/>). These porous microspheres play an important role in numerous applications, such as microscaffolds, which have specific chemicals grafted, immobilized or stored, for either a targeted effect by contact [4] or by controlled release. They are prepared by microemulsion techniques combined with the sol-gel method and their morphology, size distribution and porosity strongly depend on the water-in-oil emulsion properties and stability. The stability of the microemulsion is the key factor for controlling those microscaffolds properties and hence the quality of those microscaffolds.

1.2. Emulsions

An emulsion consists of two immiscible liquids, with one dispersed as small droplets in the other liquid. The emulsion can be classified according to the relative distribution of the different phases. An emulsion consisting of oil droplets dispersed in an aqueous phase is referred to as an oil-in-water (OW) emulsion (Figure 1a), for example, mayonnaise. An emulsion that consists of water droplets dispersed in an oil phase is referred to as a water-in-oil (W/O) emulsion (Figure 1b), for example, butter. The liquid inside the droplets is usually called the “dispersed phase”, “discontinuous phase” or “internal phase”, whereas the surrounding liquid is called the “dispersing phase”, “continuous phase” or “external phase”. The terms “dispersed phase” and “continuous phase” will be used throughout this thesis. There are also multiple emulsions of different types, such as oil-in-water-in-oil (OW/O) (Figure 1c) and water-in-oil-in-water (W/O/W) [2, 3] (Figure 1d). The process of converting oil and water into an emulsion is known as “homogenization”. This process is usually done by applying intense stirring to the mixture, involving high shear stresses, with a device known as “homogenizer”.

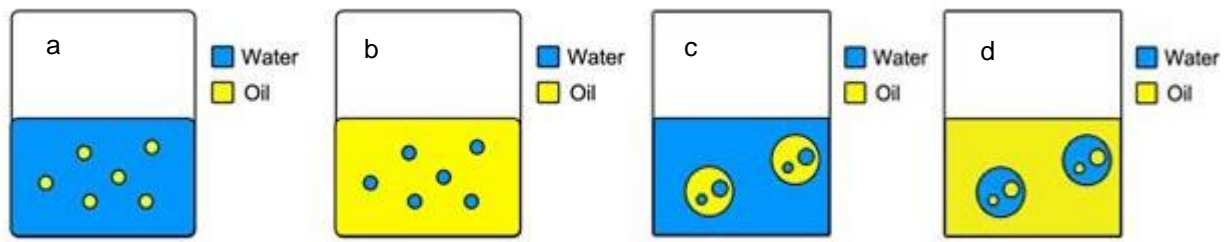


Figure 1 – Pictorial representation of the different types of emulsions. a) oil-in-water, b) water-in-oil, c) water-in-oil-in-water, d) oil-in-water-in-oil

To evaluate an emulsion, it is important to know its type and characteristics, such as viscosity, droplet size, droplet size distribution, and stability.

Regarding the destabilization process of emulsions, before the complete separation of both phases, there is a series of phenomena that may occur depending on the type of interaction of the droplets with the water or oil phases.

In the majority of cases instead of a single droplet size (monodisperse droplet size distribution), there is a distribution of different droplet sizes (polydisperse droplet size distribution). The droplets can move in the continuous phase and, since they are not rigid spheres, they can aggregate and coalesce, leading to the segregation of one of the phases or in the worst-case scenario, to the full separation of the two phases. Attractive forces pull the droplets together as repulsive forces push them apart and increase stability.

The emulsion viscosity is a measure of the resistance to the movements of the droplets. The higher the viscosity of the continuous phase, the slower the droplets would move and, therefore, the higher the emulsion stability. The droplet size plays also an important role: bigger droplets and droplets that are closer to each other favor the aggregation and could lead to instability. [2, 3]

Instability of emulsions

The most typical instability mechanisms are creaming, sedimentation, flocculation, Ostwald ripening, coalescence, phase separation, and phase inversion.

Creaming occurs when the dispersed phase has a lower density than the continuous phase and moves upward, resulting in a thick separated layer at the top of the emulsion. Creaming is not an actual breaking but a separation of the emulsion into two emulsions, one of which (the cream) is richer in the disperse phase than the other. Creaming is the principal process by which the disperse phase separates from an emulsion and is typically the precursor to coalescence.

Sedimentation is the opposite effect, since the dispersed phase has a higher density than the continuous phase, the droplets tend to move downward, resulting in a thick separated layer at the bottom of the emulsion. The velocity of creaming or sedimentation could be calculated using the Stokes Law (1), where the velocity, V_{Stokes} , depends on the density, ρ , of the two phases, the radius of the dispersed droplets, r , the shear viscosity of the continuous phase, η , and gravity acceleration g . [2, 4, 5]

$$V_{Stokes} = \frac{2gr^2(\rho_2 - \rho_1)}{9\eta_1} \quad (1)$$

Flocculation occurs when the equally larger-sized droplets gather close to one another without merging into bigger ones while remain as separate entities. Flocculation could be classified into two categories, Brownian movements' aggregation, and sedimentation aggregation.

In sedimentation aggregation, droplets of different size move up or down at different rates, depending of their density and this leads to a tendency for the faster droplets to collide with and possibly caught smaller droplets. Brownian aggregation is the result of random Brownian movement of the droplets.

It is possible to have an estimate of the relative rates of each type of flocculation movement using equation (2).

$$\Gamma_{max} = 2\pi (\rho - \rho_0) g r^4 / 3 k_b T \quad (2)$$

T is absolute temperature in Kelvin, k_b is the Boltzmann constant. ρ is the density of the droplet, ρ_0 is the density of the continuous phase, g , gravity acceleration, r is the droplet radius.

Flocculation may also occur when the smaller droplets move faster than the bigger droplets, the bigger droplets are pulled due to forced convection or by gravity. [5, 6]

Ostwald ripening is the process in which the droplets size inside an emulsion, progressively changes to larger sizes. It can be seen as a precursor to coalescence, where there are still small droplets, but they do not completely merge with the bigger ones. It is dependent on the diffusion of the disperse phase on the continuous phase. The diffusion rate can be calculated by the Stokes-Einstein equation (3).

$$D = k_b T / 6\pi\eta r \quad (3)$$

D is the diffusion coefficient of a droplet, k_b is the Boltzmann constant, T is absolute temperature in Kelvin, η is the continuous phase viscosity and r is the droplet radius. [7]

Coalescence is the process where the small droplets fully merge into bigger droplets.

Phase Separation is the complete separation of the two phases. Phase inversion is when the disperse phase becomes the continuous phase and vice-versa. [8].

In (Figure 2) the emulsion evolution and the main instability mechanisms are represented. It should be noticed that when creaming or sedimentation start to occur, there is still a small layer of emulsion present, not shown in the figure, before all the droplets completely move upward or downward.

Water and oil do not form an emulsion just by mixing and stirring as they rapidly separate as two distinct phases. So, in order to maintain the droplets from coalescing, the presence of another compound, called stabilizer, is required.

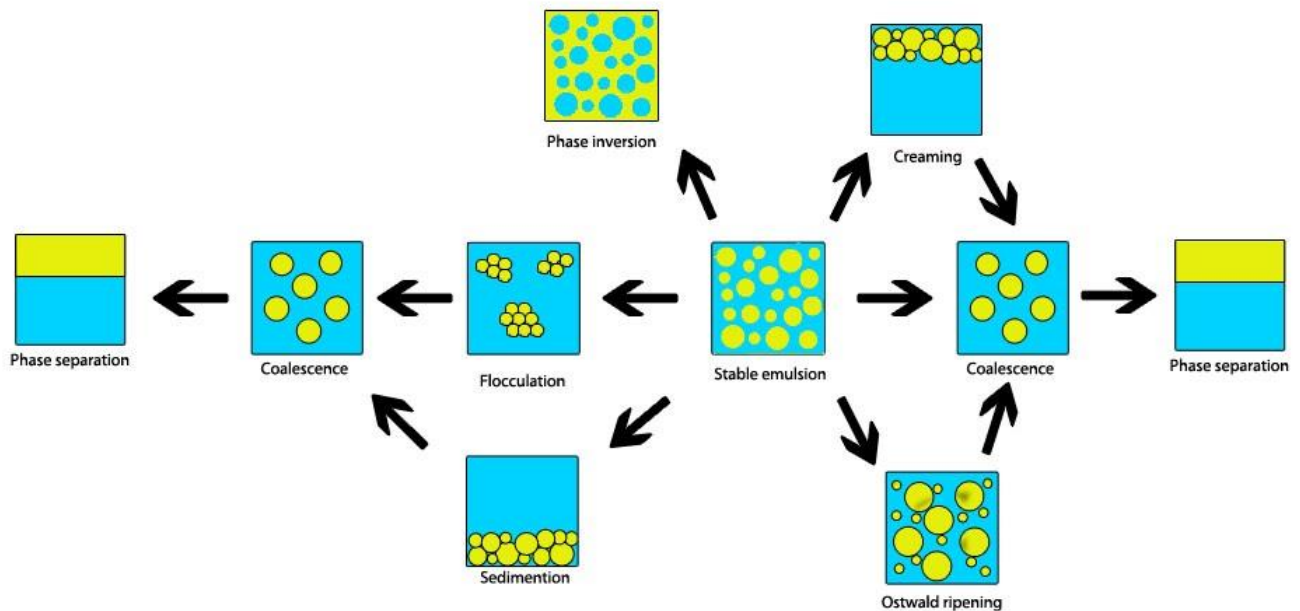


Figure 2 – Pictorial representation of the emulsions instability mechanisms.

Emulsion stabilizers

It is necessary that the emulsion remains stable over a certain period of time depending on its application. For example, in the food industry, emulsions are used to produce some products like coffee creamers, mayonnaise, and ice-cream. Therefore, it is required that the emulsion remains stable over at least the product's shelf-life.

As discussed before, the system requires the incorporation of other substances known as stabilizers. Stabilizers can be defined in two classifications, "emulsifiers" or "texture modifiers". A texture modifier

is a substance that either increases the viscosity of the continuous phase (“thickening agent”) or forms a gel network within the continuous phase (“gelling agent”). Some examples are starch and cellulose. Therefore the droplets movements become slower and it is harder for them to come closer to each other which increases the emulsion’s stability.

An emulsifier is a surface-active substance that adsorbs to the surface of the emulsion droplets, to form a protective coating that prevents the droplets, from aggregating with one another. It also reduces the interfacial tension and facilitates the disruption of the bigger droplets during homogenization. Some examples of emulsifiers are proteins, solid particles, and small molecule surfactants. [1]

Surfactants

The most used stabilizers are called surfactants. Surfactants are essentially molecules with an amphiphilic structure, meaning with both a hydrophilic group and a hydrophobic group. The hydrophilic group usually is an ionic or polar group and the hydrophobic group usually is a long hydrocarbon chain. Therefore, while in the emulsion, the surfactant molecule tends to place itself at the interface water-oil in order to satisfy both affinities. The hydrophilic side turns towards the water and the hydrophobic side turns towards oil. (Figure 3a) The way the molecule places itself on the interface will depend on the type of the emulsion and the predominance of each affinity over the other. (Figure 3b and c).

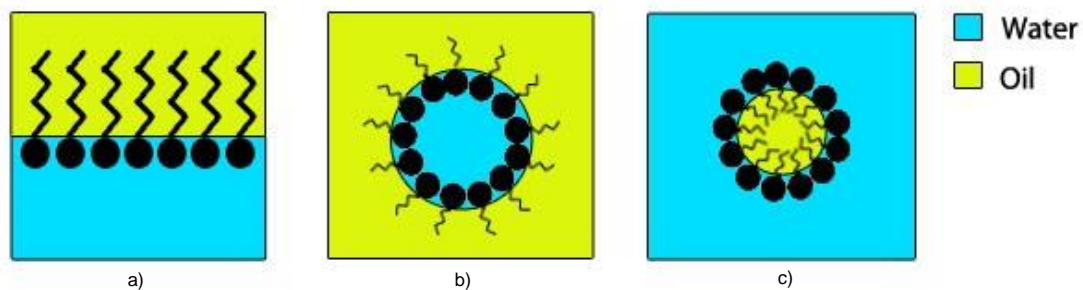


Figure 3 - Schematic representation of the distribution of a surfactant in the water/oil interface of an emulsion. a) the oil-water interface, b) on a W/O emulsion and c) on an O/W emulsion

The surfactant acts on the interface or droplet surface and has the ability to change the free energy of one or all the surfaces or interfaces of the system. The free energy of the interface could be described as the minimum amount of work required to create the interface.

So, it is possible to know the interfacial tension between the two phases as a measure of interfacial free energy per unit area equation (4). It can also be a measure of the difference of pressure of two phases at the interface, equation (5). [9]

$$\Delta G = \gamma \times \Delta A \quad (4)$$

ΔG is the interface free energy in Nm/J; ΔA is the total interfacial area of the disperse phase in m²; γ is the interfacial tension in N/m.

Therefore, the surfactant acts by lowering the interface free energy and by that lowering the surface tension, and finally decreasing the pressure difference on the drop interface, equation (5). [9]

$$\Delta P = \gamma \times (1/R_1 + 1/R_2) \quad (5)$$

ΔP is the interface pressure difference of the droplet in Pa; R_1 and R_2 is the droplets radius of curvature in m; γ is the interfacial tension in N/m.

A perfect round droplet occurs when $R_1 = R_2 = R$ equation (6).

$$\Delta P = 2 \gamma / R \quad (6)$$

One example of a surfactant is sorbitan monooleate known as SPAN 80, which is the one currently employed in the synthesis of the porous microspheres. (Figure 4)

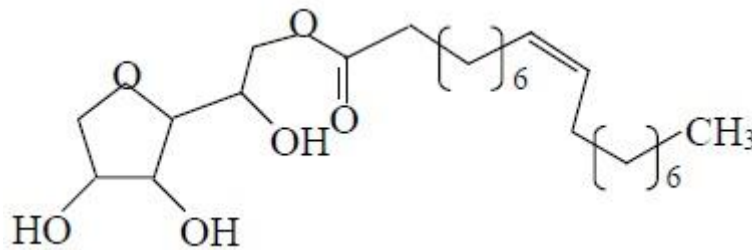


Figure 4 – Molecular structure of SPAN 80

Surfactant efficiency

Even though surfactants have an amphiphilic structure, they could have more affinity for either hydrophilic or hydrophobic. A method to know this affinity is to determine the Hydrophilic-Lipophilic Balance or HLB.

The HLB is a characteristic of the surfactant and it is a value of the relative affinity of the hydrophilic and hydrophobic groups. Its value is a ratio between the effects of the two groups. A way to find the HLB is by using the same process as William Griffin back in 1949. Griffin started by making a surfactant fully hydrophobic, oleic acid and one fully hydrophilic, sodium oleate. He gave the random values of 1 and 20 to oleic acid and the sodium oleate respectively. By mixing known quantity of each component, the HLB could be calculated based on those quantities, then tested in a water and oil solution. [3, 10, 11]

Most of the commercial surfactants have HLB tested by the same process, where they are compared to a reference sample. High values, above 10, indicate a surfactant with more affinity to water based phases, better suited for O/W emulsions. On the contrary, values below 10 indicate a surfactant with more affinity to oil based phases, hydrophobic solutions, better suited for W/O emulsions. Therefore, the HLB is a good indication about the emulsifying behavior but lacks information about the efficiency. Different surfactants within the same range of the HLB will have different efficiencies on the same system, just by changing the oil-water ratios. However the HLB could still be used as a first approach when choosing a surfactant to use in a certain type of emulsion. [3, 10, 11]

Table 1 – HLB values range and typical uses [10]

HLB	Range Use
4-6	W/O emulsifiers
7-9	Wetting agents
8-18	O/W emulsifiers
13-15	Detergents
10-18	Solubilizers

1.2.1. Stability Studies

To assess the emulsion stability, various studies can be done, focusing on the different characteristics of the emulsion. As discussed above, most instability mechanisms depend on the droplets and their coalescence tendency, therefore a method to study the emulsion stability could be the study of the droplet size and distribution.

The stability increases with smaller and more homogenous dispersed droplets, so it is possible to study the stability by changing parameters such as stirring speed, stirring time and observing the droplet size and distribution over a certain period. For example, a change in stirring speed can lead to a different size of droplets and alter the visual aspect of the emulsion in a way that can be seen to the naked eye. By using a microscope, it is also possible to see the droplets inside the emulsion and determine its size and distribution. [2, 12–14]

1.2.2. Pickering Emulsion

As discussed before, solid particles could be used to stabilize an emulsion, being those emulsions that utilize solid particles instead of a surfactant called Pickering [15] emulsions.

The main advantages of using solid particles instead of a surfactant are the reduced possibility of coalescence and the fact that solid particles can be made of a specific material or can be functionalized, in order to be tailored for specific applications.

The common mechanism of stabilization is the formation of a barrier by the adsorbing particles at the water-oil interface. The emulsion formed is determined by the wettability of the particles, i.e. if one of the liquids wets the particles more than the other, the liquid which wets the particle better becomes the continuous phase and the other liquid becomes the dispersed phase. In solid particles, this is determined by the three-phase angle, θ . If the contact angle is above 90° (Figure 5a), it should form a W/O emulsion, if the angle θ is less than 90° (Figure 5c), it should form an O/W emulsion. But ideally, to maintain the stability, the angle θ should be close to 90° (Figure 5b) so the particles remain in the interface, instead of dispersing in either of the phases. [16, 17] Usually, these amphiphilic particles are obtained from the most common particles and modified to a certain degree, such as silica, clay, hap, chitosan, and others.

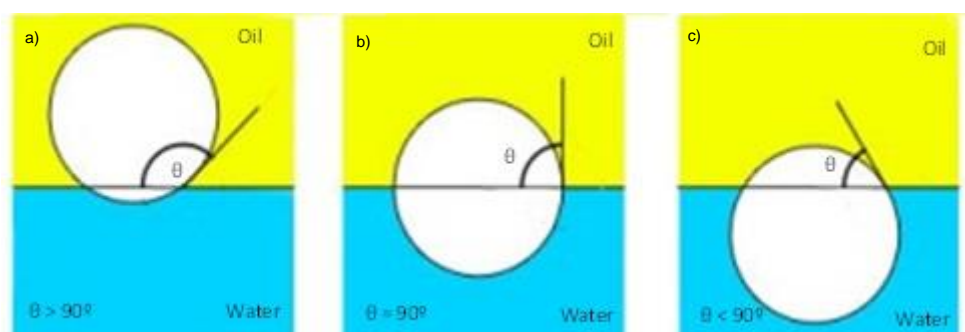


Figure 5 - Schematic of a solid particle in the water-oil interface. a) Particle in oil phase – hydrophobic, b) particle in the interface – amphiphilic, c) particle in the water phase - hydrophilic.

To understand the particle behavior on the emulsion, it is required to characterize it. One of the most used material in Pickering emulsions is silica. Silica particles are easily obtained and modified. Many experiments [18–21] indicated that unmodified silica tends to stabilize O/W emulsions due to the hydrophilicity resulting from Si-OH groups on the particle surface, while hydrophobically modified silica preferentially stabilizes W/O emulsions. Indeed, unmodified silica particles, hydrophilic in character, have been successfully used for emulsification of polar oils, while modification of the silica surface also enables emulsification of non-polar oils. [22]

The common particle size used for Pickering is variable. In some cases, example of starch, it is possible to produce particles in the order of magnitude of 100-200 nm. [23]. While in others cases, it particles up to 30 μm [24], or with 0.6 - 1.2 μm can be employed. [25]

1.3. Hybrid porous microspheres

As referred before, the silica hybrid porous microspheres are possible to be synthesized by using the sol-gel process combined with emulsion techniques. The “sol” is a colloidal suspension that leads to the formation of a “gel”.

The sol-gel process undergoes four steps (Figure 6):

1st) Silane pre-hydrolysis

An alkoxy silane precursor is hydrolyzed, forming hydroxides species. The alkoxy groups (OR) are replaced with OH groups. The most important parameters in the pre-hydrolysis is the catalyst concentration, i.e. the solution pH. However, some other parameters may influence the reaction such as the solvent, the molar ratio of water to silane and temperature. [26, 27]

The presence of a catalyst is not essential as the hydrolysis still occurs, but by using the catalyst, the speed and degree of conversion will be maximized. The catalyst can be either basic or acidic. The hydrolysis rate has a minimum at pH 7 and increases, either with the increase of pH while using a basic catalyst, or the decrease of the pH while using an acidic catalyst. However, for equivalent conditions, the acidic catalysis is faster.

In the acidic hydrolysis, the alkoxy group will be protonated and therefore available to react with water. [26, 27]

In the basic hydrolysis, the hydrolysis reaction will likely begin by dissociating water to produce hydroxyl anions, and then the ions react with the silicon atom. This step is slower than the acidic hydrolysis because of some repulsion between the oxygens of the alkaloid and the OH nucleophilic. [26]

2nd) Hidroxysilane (silanol) condensation

Oxides species are formed in a condensation reaction. The Si-OH group from the first step will lead to the formation of Si-O-Si siloxane bounds, with the production of byproducts alcohol or water, depending on the type of condensation. [26–28]

As time advances the number of siloxane bounds increases and more individual molecules aggregate in the “sol” to start forming a network. Usually, the condensation begins before the end of the pre-

hydrolysis, but within certain conditions such as pH, silane to water ratio and/or catalyst, it is possible to fully complete the hydrolysis before the condensation occurs. [26]

In the same way as in the pre-hydrolysis, the use of a catalyst is not essential. But once again, it will increase greatly the speed of the reaction. The catalyst can be either basic or acidic with a minimum rate at pH 2 and increases with the increase in the pH until pH 7, then decreases to pH above 7, for siloxane formation. [27–29]

3rd) Gelation and aging

The gelation is the change in properties that occur in the sol while it changes into a gel. Clusters formed in the first and second step, collide, start to form links and combine into a single cluster, to be called a gel. As the clusters combine, the stiffness of the gel increases until the last link is formed.

After the gelation, comes the aging step. In the aging process, changes occur in structure and properties. There is the formation of crosslinks, making the network stronger and stiffer. [26, 27]

4th) Drying.

Since there is still water, alcohol or other volatile components present, is necessary to remove them from the system, by drying. If the material has pores, the process starts by evaporating the liquid at the surface causing the body to shrink. When it cannot shrink anymore, the liquid goes to the interior, but there is still a film of liquid at the interface allowing the flow to the exterior and therefore the evaporation at the surface continuous. In the last phase, only the liquid inside remains, so drying occurs by evaporation inside the body while the vapor flows to the outside. [26, 27]

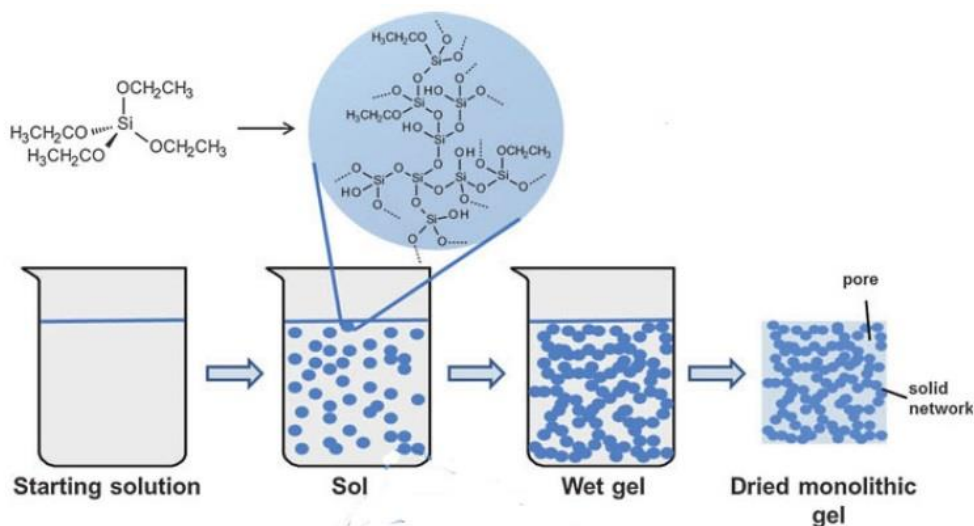


Figure 6 - Schematic representation of the sol-gel process [31]

The two alkoxysilanes that are used as precursors in the sol-gel process for the synthesis of the porous microspheres are tetraethyl orthosilicate (TEOS) and (3-glycidyloxypropyl) trimethoxysilane (GPTMS). (Figure 7)

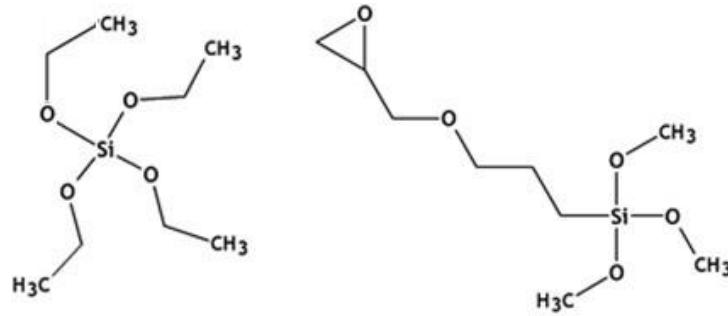


Figure 7 – Molecular structure of TEOS (left) and GPTMS (right)

1.4. Silica submicron particles by a modified Stöber method

The Stöber process (Figure 8) is a process to create silica particles based in the sol-gel process, described above.

In 1968 Stöber et al [32], initiated a study to evaluate the physicochemical properties and effects of colloids and aerosols at that time. During his investigation about the possibilities of producing monodisperse suspensions of silica spheres, he synthesized silica particles from silicon alkoxysilanes in an alcoholic solution, using ammonia as a catalyst.

His work showed that by changing the ratios of the components in the mixture, the size of the particles could be controlled, in the range of 50 nm to 1 μ m diameters. This innovating method proved to be a foundation for colloid synthesis field of research, as it possible to obtain small silica particles with a homogenous distribution with low cost and control of the particle size.

Later studies like [33], were able to modify and improve the synthesis in terms of knowledge about its final yield and factors. Later works study the effect of the concentration of a salt in the solution [33], on the size of the particles.

The process occurs as the following:

First, the alkoxides are hydrolyzed and the OR groups are replaced with a group OH, releasing the respective alcohol or water depending on the type of condensation.

The Si – OH bond is broken releasing water, as more Si-O-Si chains start to form.

As time advances more and more crosslinks occur and more alkoxides agglomerate, the network progressively increases and occurs the formation of the “gel”.

Final the gel is dried to remove any water, alcohol or other volatile components.

The size of the particles will vary with the concentration of TEOS in relation to concentrations of water and ammonia in ethanol.

The process can be done in either one step or two steps, one step if the condensation step occurs before the end of the hydrolysis or two steps if the if the condensation step occurs after the hydrolysis. The two steps advantage is the more control over the process as the hydrolysis and condensation steps are separated.

The main advantage when comparing with the sol gel process, is the smaller dimension of the particles and the more control over the synthesis process.

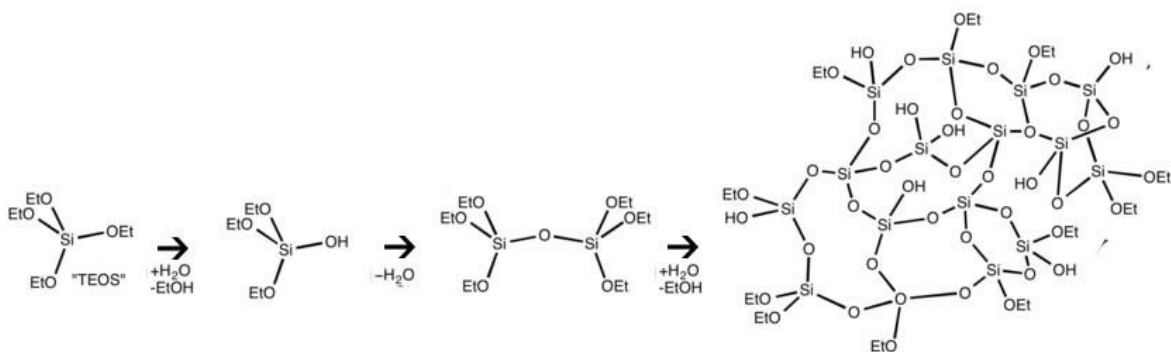


Figure 8 - Schematic representation of the Stober process using TEOS as Si precursor

1.5. Hydrophobic treatment

Silica particles are hydrophilic because of the Si-OH groups on their surface. In order to obtain silica hydrophobic particles, it is necessary to modify their surface.

The approach used in this work is based on Hexadecyltrimethoxysilane (HDTMS) due to its long hydrocarbon chain.

The process can be done, either by using HDTMS as Si “hydrophobic” precursor and mix it with other precursors, such as TEOS, in a synthesis process, obtaining hydrophobic particles (bottom-up approach), or by using HDTMS as a coating agent that will modify the particles surface.

In this latter approach, the Si-O-CH₃ groups of HDTMS will hydrolyze, forming silanols that condense with silanols at the surface of the silica particles, forming a link composed of siloxane units. The long hydrocarbon chain gives the particles the required hydrophobicity character. (Figure 9) [34–41]

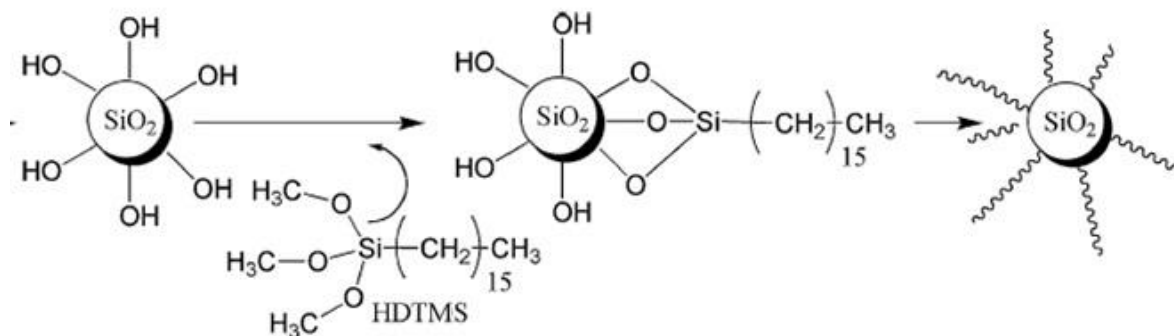


Figure 9 – Schematic representation of the hydrophobic treatment process [34]

1.6. Objective and work strategy

In The main goal of the present work is the development of submicron particles, to be used as emulsion stabilizers in the current synthesis protocol of the porous silica hybrid microspheres. Having this into account, the following steps were carried out:

1st) optimization of the porous silica hybrid microspheres synthesis.

The process used is the sol-gel process because it enables the control of the structure of the particles, as well as their shape and size by carefully choosing the operational parameters. [28] Therefore, in order to optimize the process, the mechanical stirring speed, the emulsification speed, and the concentration of the surfactant were varied to study their effect. The resulting particles were compared, and the optimal conditions were identified, after characterization of the particles by Fourier transformed infrared spectroscopy and by scanning electron microscopy.

2nd) synthesis of submicron silica particles.

The particles prepared were made of silica because their synthesis and surface modification is relatively straightforward [18–21]. The process chosen [42] was a modified Stöber process, since it requires a low amount of reactants and employs low toxicity reactants. The particles were characterized by Fourier transformed infrared spectroscopy and by scanning electron microscopy. In

order to make the submicron particles more suitable for water-in-oil emulsions, the selected particles were subject to a hydrophobization treatment using HDTMS

3rd) evaluation of the stability of the emulsions

Different types of submicron particles, at different concentrations were used in these studies. The current emulsion, W-in-O (O=decalin) stabilized with SPAN80, was used as a reference. Another emulsion, using Pluronic P123 as surfactant, was also included in the tests to check the effect of a different surfactant. These surfactants were added at different concentrations. The strategy employed to evaluate the emulsions' stability was by direct observation (by naked eye), which allows to evaluate the macroscopic instability phenomena occurring along the time, and by observation using an optical microscope to evaluate the droplets behavior, and their size distribution along the time. The volume fraction of the emulsion phase that remains along the time was monitored.

2. Experimental Section

2.1. Materials

A description of the compounds used and some of their properties are described in Table 2 and Table 3.

Table 2 – Compounds used and their suppliers

Classification	Compound	Common name	CAS	Manufacture
Silanes	Xiameter OFS-6697	TEOS	78-10-4	Dow Chemical (former Dow Corning)
	Xiameter OFS-6040	GPTMS	2530-83-8	Dow Chemical (former Dow Corning)
	Hexadecyltrimethoxysilane	HDTMS	16415-12-6	Aldrich
Catalysts	Hydrochloric acid 37%	HCl	7647-01-0	Carlo-Erba
	Ammonia solution 25%	Ammonia	1336-21-6	Merck
Surfactants	SPAN® 80 for synthesis	SPAN 80	1338-43-8	Merck
	Poly(ethylene glycol)- <i>block</i> -poly(propylene glycol)- <i>block</i> -poly(ethylene glycol)	Pluronic P123	9003-11-6	Sigma-Aldrich
Solvents	Deionized water	Water	7732-18-5	MiliQ
	Decahydronaphthalene	Decalin	91-17-8	Merck
	Ethanol, absolute	Ethanol	64-17-5	Fisher Scientific
Salts	n-Hexane	n-Hexane	110-54-3	Merck
	KCl	KCl	7447-40-7	Merck
Silica commercial particles	HIPRESICA SS N3N 1 µm	N3N1 ^(a)		UBE EXSYMO CO., LTD,
	HIPRESICA TS N3N 3 µm	N3N3 ^(a)		UBE EXSYMO CO., LTD,
	HIPRESICA TS N6N 3 µm	N6N3 ^(a)		UBE EXSYMO CO., LTD,
	HIPRESICA FQ N2N 0.2 µm	N2N ^(a)		UBE EXSYMO CO., LTD,

^(a)these references were used throughout this thesis for simplicity purposes.

Table 3 – Physical and chemical properties of the compounds employed

	Grade (%)	ρ (g/cm ³)	Viscosity (mPa.s)	B.P. (°C)
TEOS	98	0.933	0.66	168
GPTMS	>98.5	1.07	0.0321	250
HDTMS	<=100%	0.89	350	180
Hydrochloric acid	37%	1.17	1.9	85
Ammonia	25%	0.903	N/A	37.7
SPAN 80	99	0.986	1000-2000	463
Pluronic P123	99	1.018	350	149
Deionized water		1	1	100
Decalin	99	0.88	3	189-191
Ethanol	>99	0.79	1.2	78
n-Hexane	98,5	0.659 - 0.663	0.30	-67 - 69
KCl	>99	1,98	-	-

2.2. Methods

2.2.1. Synthesis of porous silica hybrid microspheres by microemulsion combined with sol-gel process

The process to make the sol-gel porous microspheres was based on a previous study [4], consisting of four steps:

- **Pre-hydrolysis**

The pre-hydrolysis was done by mixing TEOS, GPTMS and an aqueous solution of HCl 0.05 M, in the proportion 1:1:0.75 (w/w), then stirring for one hour, in a closed cup, using a magnetic stirrer, at room temperature.

At 10 minutes before the end of pre-hydrolysis, it was added 300 µl of HCl at 37%.

The HCl 0.05M solution was done by using deionized water and HCl at 37%.

- **Emulsification**

The emulsion was prepared by mixing decahydronaphthalene, and SPAN 80, in the proportion 100:6 (w/w), then stirring for 3 minutes at various speeds using an IKA Ultra Turrax T-18. This was followed by adding 45 g (wt% relative to decahydronaphthalene) of water and stirring for more 10 minutes at the same speed.

The start time of the emulsion was timed in order to start 13 minutes before the end of the pre-hydrolysis, to ensure that the emulsification and the pre-hydrolysis processes end exactly at the same time.

The stirring speed at the emulsification process and the amount of SPAN were varied according to Table 5.

- **Reaction**

The emulsion was then placed inside a reactor in a heating mantle, just keeping the temperature ca 25 °C. After, the emulsion was stirred at 600 rpm and the pre-hydrolyzed solution was added to the reactor dropwise, followed by a specific temperature/time profile, as shown in

Table 4.

Table 4 – Steps of temperature employed in the synthesis

T (°C)	Time (min)
Room temperature (ca 25)	60
65	60
70	10
75	15
80	60
85	60
90	60
95	60

- **Filtering and drying**

The reaction product was then filtered under vacuum, using n-hexane as a solvent. The wet particles were placed in an oven to dry at 45 °C overnight, to evaporate the water and other volatiles.

In order to optimize the syntheses parameters, the following tests were carried out, according to Table 5.

Table 5 – Sol-gel synthesis operational conditions and samples

Samples	Speed of emulsification (rpm)	Speed of mechanical stirring in the reactor (rpm)	Quantity of surfactant, in g (wt% of the organic phase)	Comments
SD23	9800	600	6	Reference conditions
SD24	9800	800	6	
SD25	13000	600	6	
SD26	18000	600	6	
SD27	18000	600	8	
SD29	18000	600	6	Repetition of SD26

SD30	9800	600	6	a)
SD31	9800	600 / 1000	6	b)
SD32	18000	600	6	Repetition of SD26

- a) The temperature in the reactor was set to 80°C from the start, then followed the procedure described above.
- b) The stirring speed inside the reactor was set at 1000 rpm until the temperature reached 75°C and then was reduced to 600 rpm when the temperature reached 80°C

The experimental procedure is schematically represented in Figure 10, Figure 11 and Figure 12.

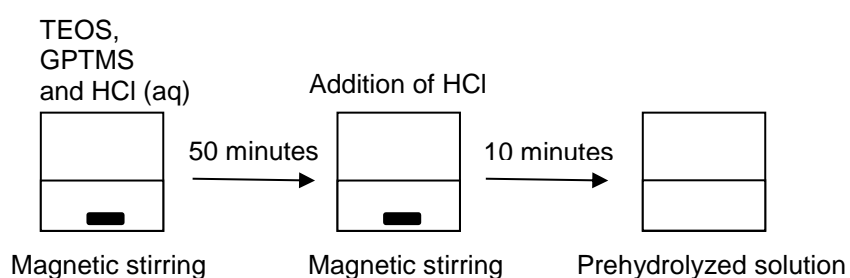


Figure 10 - Schematic representation of the pre-hydrolysis step

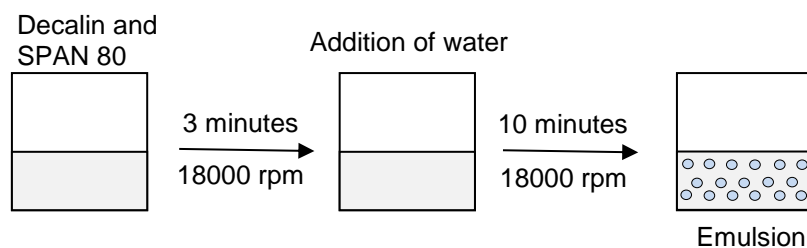


Figure 11 - Schematic representation of the emulsification step

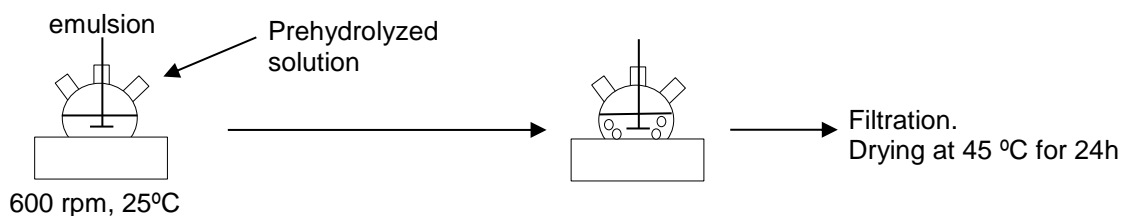


Figure 12 - Schematic representation of the synthesis, filtration and drying steps

2.2.2. Characterization of the porous silica hybrid microspheres

The particles were characterized under scanning electron microscopy (TEOS), using the JEOL JSM-70001F Field Emission Scanning Electron Microscope and Fourier transformed infrared spectroscopy (FTIR) using a PerkinElmer, Spectrum Two, FTIR spectrometer equipped with a Pike Technologies Miracle® ATR accessory at 4 cm⁻¹ resolution and 4 scans of data accumulation.

2.2.3. Synthesis of silica submicron particles by a modified Stöber method.

The process to make the submicron silica particles is based in four stages as indicated in [42].

- Preparation of solution I

The following compounds were mixed in a plastic container: 0,0238g of KCl, 9,45g of ethanol, 1,648g of TEOS and 4 ml of an aqueous solution of ammonia (25%). After that, the solution was placed in a glass reactor at 35°C under mechanical stirring at 240 rpm for one hour.

- Preparation of solution II

26,12g of ethanol and 4,12g of TEOS were mixed in a plastic container.

- Reaction

According to reference [42].

Solution II should have been added to the reactor, using a pump at a constant rate. Due to the lack of such pump, the process was modified by adding the volume equivalent to an hour, in a hour by hour basis. This volume was calculated as the total volume required divided by the number of hours of reaction. After adding all the solution II to the reactor, it was left stirring for one hour more.

The profile of solution II addition was set according to Table 6.

Table 6 – Feeding profile of solution II to the reactor

Time Hour number	Volume added (ml)
0	0
1 st	6
2 nd	6
3 rd	6

4 th	6
5 th	6
6 th	7,66
7 th	0

- Centrifugation

At the end of the reaction, the content from the reactor was retrieved to a vessel and subject to centrifugation at 7000 rpm using a centrifuge Sigma Sartorius 4-16 for 5 minutes and washed with ethanol, repeating the cycle two times. The vessel was then placed in an oven at 60°C overnight to evaporate all the ethanol and other volatiles.

In order to obtain a good amount of sample to proceed with the studies and to evaluate the reproducibility of this method, all process was repeated and the particles compared. The following syntheses were done according to Table 7.

It should be noted that syntheses SD 46 and 48 were done to evaluate the effect of the salt concentration on the particles aggregation.

Table 7 – Stöber modified process samples

Samples	Operating conditions
SD28	Set as reference, using the conditions described above
SD34	Scale-up by 200%
SD36	Same conditions
SD39	Same conditions
SD40	Same conditions
SD42	Same conditions
SD44	Same conditions
SD46	84% of original KCl mass
SD48	92% of original KCl mass

The experimental procedure is schematically represented in Figure 13.

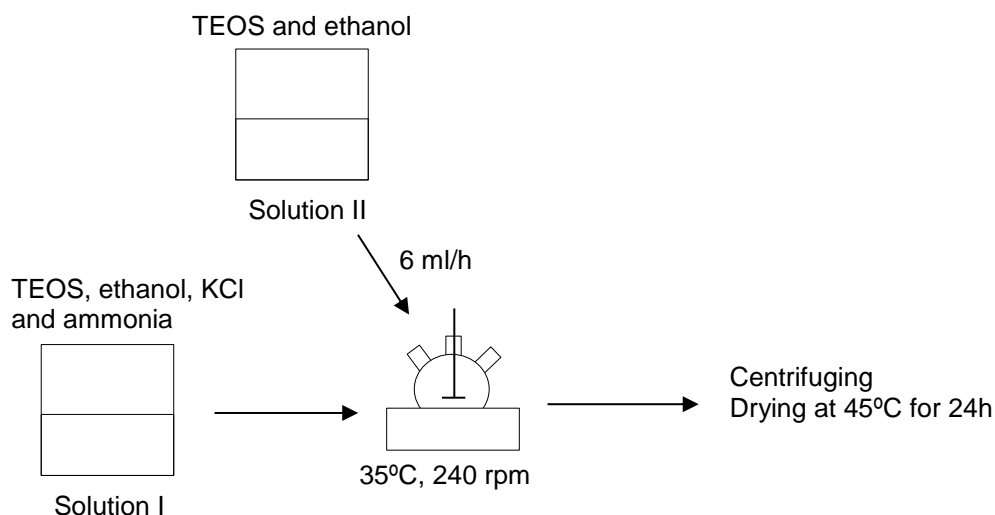


Figure 13 - Schematic representation of the synthesis of silica submicron particles

2.2.4. Characterization of silica submicron particles

The particles were characterized using SEM microscopy, using the JEOL JSM-70001F Field Emission Scanning Electron Microscope and FTIR using a PerkinElmer, Spectrum Two, FTIR spectrometer equipped with a Pike Technologies Miracle® ATR accessory at 4 cm^{-1} resolution and 4 scans of data accumulation.

2.2.5. Characterization of silica commercial particles

The particles kindly supplied by a Japanese company, UBE EXSYMO CO., Ltd., were also characterized under SEM, using the JEOL JSM-70001F Field Emission Scanning Electron Microscope.

2.2.6. Hydrophobic treatment

The following hydrophobization process was carried out:

50 ml of distilled water was acidified to pH 3 using HCl at 37%. Then 0,562 ml of HDTMS was added to the acidic aqueous solution and stirred at 300 rpm for 1 hour at 50 °C. After 1 hour, a certain amount of particles were placed in the mixture and stirred for 30 minutes at 300 rpm and 50°C. After 30 minutes the mixture was centrifuged at 5000 rpm for 5 minutes. The remaining solid was placed in an oven at 60°C to dry out the remaining water and other volatile components.

It should be noted that the samples subjected to this treatment have an “H” in their acronym. E.g. SD36 becomes SD36H, throughout the entire thesis.

2.2.7. Characterization of silica hydrophobic particles

The particles were characterized using SEM, using the JEOL JSM-70001F Field Emission Scanning Electron Microscope and FTIR using a PerkinElmer, Spectrum Two, FTIR spectrometer equipped with a Pike Technologies Miracle® ATR accessory at 4 cm⁻¹ resolution and 4 scans of data accumulation.

2.2.8. Emulsion stability studies

The W/O emulsion used in these studies was composed of decahydronaphthalene (decalin) as the organic phase and water, with a decalin to water ratio of 10:4,5. To better distinguish the two phases a blue coloring agent was added to the water phase. The objective was to evaluate the stability of the emulsion by observing the visual aspect (by naked eye) of the emulsion along the time, as well as the evolution of the emulsion droplets size distribution by using an optical microscope.

Stability studies involving surfactants

The effect of two different surfactants on the emulsion stability was carried out using SPAN 80 and Pluronic P123. Decahydronaphthalene together with the surfactant, at variable concentration, were mixed and stirred at 18000 rpm during 3 minutes by using an IKA Ultra Turrax T-18. After 3 minutes, water was added and the mixture was stirred for more 10 minutes. After 10 minutes, the emulsion was placed in a test tube.

Table 8 lists the different tested combinations.

All the samples were placed side by side and observed at regular periods of time, by naked eye and using an optical microscope. During the observations, a photo of the emulsions in the tubes was taken using a Fujifilm FinePix S5700 with autofocus.

Table 8 - Surfactant test samples

Sample	Surfactant used	Quantity (wt% of organic phase)
S2	SPAN 80	2
S4	SPAN 80	4
S6	SPAN 80	6
S8	SPAN 80	8
P2	Pluronic P123	2
P4	Pluronic P123	4
P6	Pluronic P123	6
P8	Pluronic P123	8
P10	Pluronic P123	10
P12	Pluronic P123	12

Stability studies involving submicron particles.

The method employed to test the particles was similar to that of the surfactants before described.

Submicron particles were added to one of the phases, according to a selected particle concentration, and sonicated for 10 minutes using a VWR ultrasonic bath. After 10 minutes, the other phase was added and the mixture was emulsified at 18000 rpm for 10 minutes by using an IKA Ultra Turrax T-18. The resulting emulsion was placed in a test tube.

The same method was followed for all the particles, according to

Table 9.

All samples were placed side by side and observed at regular periods of time, by naked eye and using an optical microscope. During the observations, a photo of the emulsion inside the test tubes was taken using a Fujifilm FinePix S5700 with autofocus.

Table 9 – Particle stability studies samples

Sample	Size (μm)	Concentrations used (wt% of organic phase)			Suspend phase (phase to which particles were added)	
SD36	0.3	0.2	2	SD36	Organic	
SD36H	0.3		0.2		Organic	
N3N1	1	0.2	2	N3N1	Organic	
N3N3	3	0.2	2	N3N3	Organic	
N6N3	3	0.2	2	N6N3	Organic	
N2N	0.2		2		Water	
N2NH	0.2	0.2	2	N2NH	Organic	

3. Results and discussion

Part I - Silica hybrid porous microspheres

3.1. Synthesis of silica hybrid porous microspheres.

The different microspheres syntheses carried out in this work had the goal of (a) optimizing the synthesis parameters, (b) reducing the size and agglomeration of the microspheres, and (c) reproducibility studies. Figure 14 shows the microspheres obtained in synthesis SD23, using “reference” parameters, namely 9800 and 600 rpm as the emulsification speed and mechanical stirring speed, respectively, and 6 g of SPAN80, as explained in the Experimental Procedure section of this thesis. Apart from the presence of particle agglomerates, that can be easily removed by sieving operations, the size distribution of the microspheres SD23 is found to be quite homogeneous, around ca. 40 μm in average. Moreover, their surface exhibits the targeted high porosity, which is a potential advantage for posterior impregnation operations, for instance.

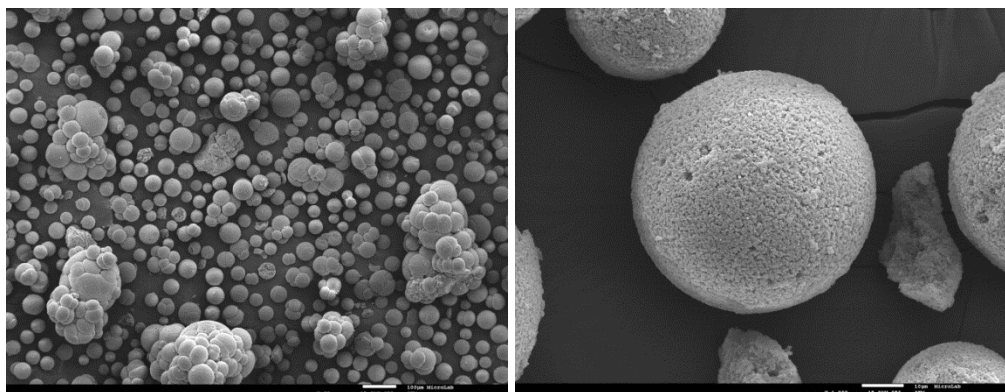


Figure 14 - SEM photomicrographs of SD23 (scale bar =100 μm at left 10 μm at right)

By increasing the reactor mechanical stirring speed, it was expected that the droplets would be smaller and would be more separated from each other.

When the speed was increased from 600 to 800 rpm, SD24, the corresponding SEM photomicrograph showed that the microspheres tend to break (Figure 15), which suggests that the stirring at 800 rpm was too much, especially at the stage when the particles are already formed with a relatively high stiffness degree.

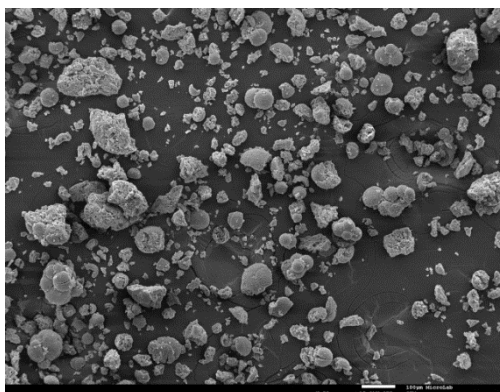


Figure 15 - SEM photomicrograph of SD24 (scale bar =100 μm)

On the other hand, the increase of the emulsification stirring speed was tested in order to lead to a decrease in the droplets size and hopefully to a more stable emulsion. Indeed, the increase in the emulsification stirring speed from 9600 rpm to 13000 rpm (SD25), and then to 18000 rpm (SD26) was found to result in a lower agglomeration of the microspheres, as can be observed in the SEM photomicrography of SD26. In fact, with 13000 rpm there was some fragmentation, but the agglomeration was reduced when comparing with SD23 (980 rpm), while with 18000 rpm, the microspheres showed no fragmentation and no agglomerations. (Figure 16)

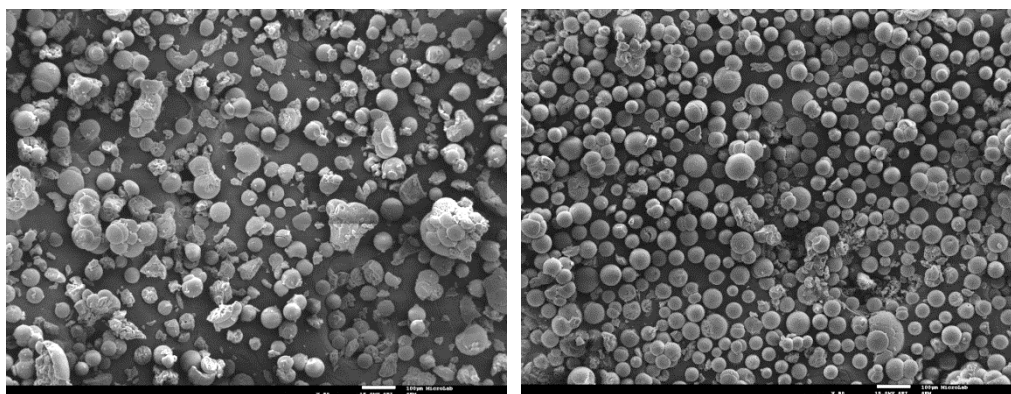


Figure 16 - SEM photomicrographs of SD25 (left) and SD26 (right) using the same magnification (scale bar = 100 μm)

Based on the above results, less agglomeration and less fragmentation for SD26, the conditions employed for SD26 were those selected to proceed with the studies.

In what regards the amount of surfactant employed in the syntheses, the increase in quantity from 6 to 8 g (wt% of organic phase) of SPAN 80 (SD27) was found to not improve the morphology of the particles. Indeed, the resulting particles (Figure 17) were very similar to the ones obtained with 6 g

(SD26), but some of the microspheres show fragmentation, therefore there were no gains in increasing the concentration, so the quantity of SPAN 80 was maintained.

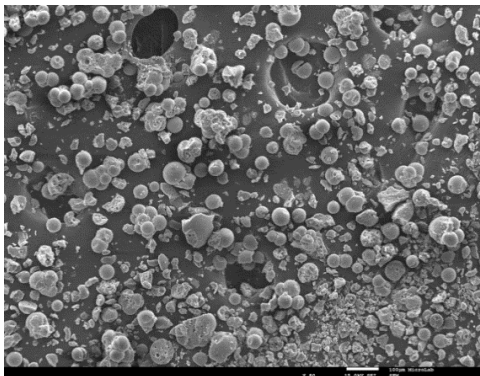


Figure 17 - SEM photomicrograph of SD27 (scale bar = 100 μm)

When the synthesis was repeated under the same conditions of SD26 there was fragmentation of some microspheres, which did not occur anymore in a second attempt. In this latter one, it was visible that the microspheres were very similar (Figure 18, right) to the ones obtained before (SD26) shown in Figure 19. So the process could be reproduced.

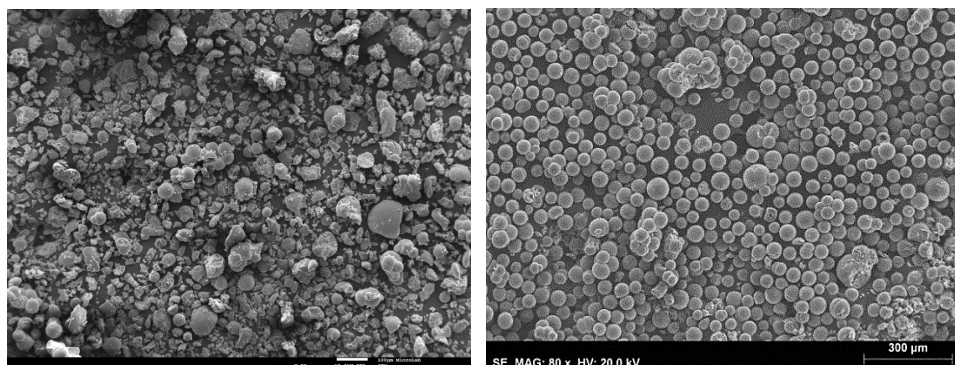


Figure 18 - SEM photomicrographs of SD29 and of SD32 (at the same magnification, scale bar = 100 μm at left 300 μm at right)

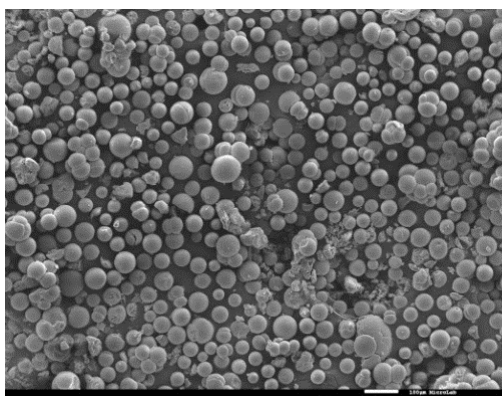


Figure 19 - SEM photomicrograph of SD26 (scale bar =100 μm)

A careful observation of the phenomena occurring during the synthesis, showed that the time taken for the reaction medium to increase its temperature from 80 to 85°C was indeed longer than the time taken to increase the temperature e.g. from 75 to 80°C. Previous works, such as that of Matsuoka et al. [43] referred a large exothermic reaction (12.9 kJ·mol⁻¹ for 1 mole of TEOS) due to the hydrolysis of TEOS, a slow exothermic reaction following it, and after that, a change of the sol-gel reaction to a small endothermic one, when condensation reactions play a major role. Indeed this might be occurring in the present work, based on the different rates of temperature increment of the reaction medium, observed during the reaction. Synthesis SD30 explored the effect of skipping some temperature steps, to check if a faster synthesis process would lead to the same result in terms of microspheres quality. The temperature in the reactor was set, in this case, to 80°C from the start, keeping the same all the remaining procedure. As Figure 20 **Erro! A origem da referência não foi encontrada.** shows, this process was found to lead to similar microspheres as in the other syntheses, but exhibiting much more agglomeration.

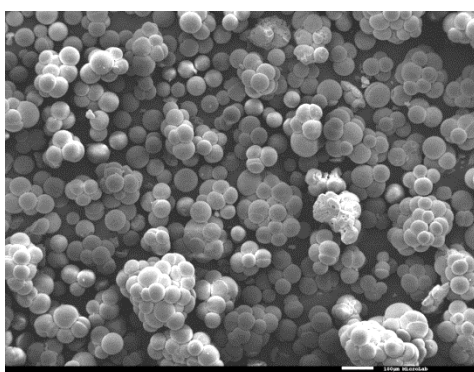


Figure 20 - SEM photomicrograph of SD30 (scale bar = 100 μm)

The synthesis SD31 was done as an attempt to avoid agglomeration by increasing the mechanical stirring speed inside the reactor, without obtaining the fragmentation seen before. For such purpose a mixed mechanical stirring speed was employed, namely 1100 rpm in a first stage, followed by 600 rpm in a later stage (when the particles start to be solid). The results (Figure 21) show the absence of fragmentation, as desired, but a very extensive aggregation of the particles.

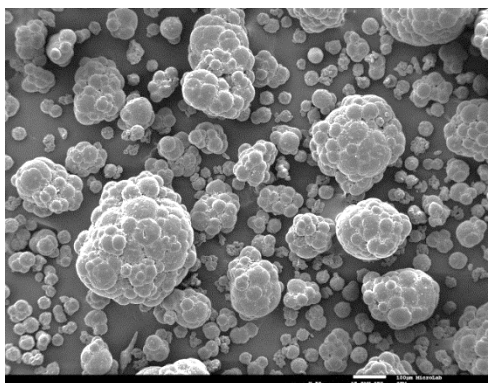


Figure 21 - SEM photomicrograph of SD31 (scale bar = 100 μm)

From the above described studies, it was concluded that the processing conditions employed in SD26 were the ones that result in the best microspheres quality, namely 18000 rpm as stirring speed in the emulsification step, 600 rpm as mechanical stirring speed inside the reactor and 6 g (w/w% of organic phase) of SPAN 80.

FTIR-ATR was employed to characterize the obtained microspheres in terms of chemical structure. Figure 22 Shows the FTIR spectrum achieved for the reference sample SD23, and it was found to be very similar to the remaining samples prepared by varying the processing conditions.

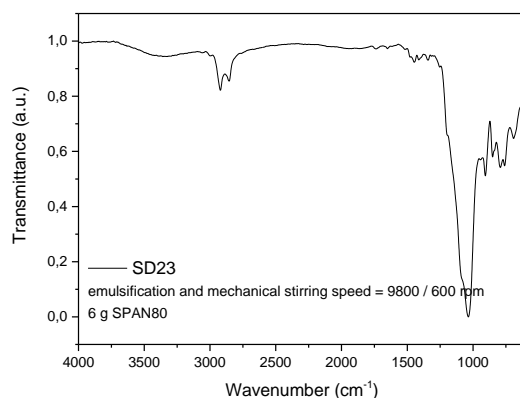


Figure 22 - FTIR spectrum of SD23

In the FTIR spectrum (Figure 22), the broadband from 3400 to 3200 cm^{-1} is relative to the stretching vibration of the O-H bond. The bands peaked at ca. 2920 cm^{-1} and 2850 cm^{-1} are ascribed to the asymmetric and symmetric C-H stretching in CH_2 groups attached to oxygen, while the band at 1450 cm^{-1} is due to the CH_3 umbrella mode, or the C-H asymmetric bending of C- CH_3 and/or C- CH_2 scissors. [44] This could be an indication of the remaining glycidyoxy organic functionality (derived from GPTMS) in the siloxane network. The high-intensity peak at 1036 cm^{-1} with the shoulder at 1200 cm^{-1} and the peak at 800 cm^{-1} correspond to the asymmetric and symmetric stretching of the siloxane

bonds (Si-O-Si) and the low intensity peak at ca. 945 cm^{-1} is ascribed to silanol Si-O stretch. It should be noted that the stretching of the C-O-C of ethers also may contribute to the intensity of the 1036 cm^{-1} peak. The peaks near 1250 cm^{-1} , 906 cm^{-1} and 859 cm^{-1} are related to C-O and C-O-C deformation of the epoxy (oxirane) group present in GPTMS. A small peak at ca. 3050 cm^{-1} can also be identified and is attributed to the C-H tension of the methylene group of the epoxy ring. The peak at ca. 765 cm^{-1} may be ascribed to the rocking of CH₂.

These results show an evidence for the hybrid character of the synthesized microspheres, in what regards silica (siloxane) moieties and glycidylloxy (epoxide) organic functionality.

Part II - Silica submicron particles for emulsion stability.

3.2. Synthesis of silica submicron particles by a modified Stöber method

Repeating several times the synthesis (based on the Stöber method) previously explained in the Experimental section, it was possible to conclude that such synthesis protocol is not straightforward in what regards reproducibility. The particles were similar, but with a varied size distribution and agglomeration in each synthesis.

Figure 23 (image on the left) shows the particles obtained in synthesis SD28, where a particle size in the range of $0.1 - 1.6\text{ }\mu\text{m}$ is observed, while particles obtained using exactly the same protocol, synthesis SD36, exhibit a very homogeneous particle size distribution, with particles of ca. $0.3\text{ }\mu\text{m}$. (Figure 23, image on the right).

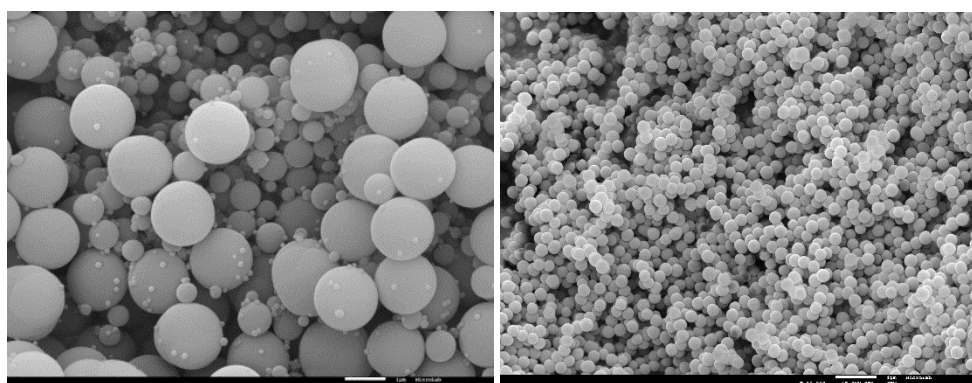


Figure 23 - SEM photomicrographs of SD28 (image on the left) and SD36 (image on the right) for the same magnification. (scale bar = $1\text{ }\mu\text{m}$)

The remaining syntheses carried out, using again the same protocol (syntheses SD39, SD40, SD42, and SD44), showed the presence of agglomeration. (Figure 24 and Figure 25)

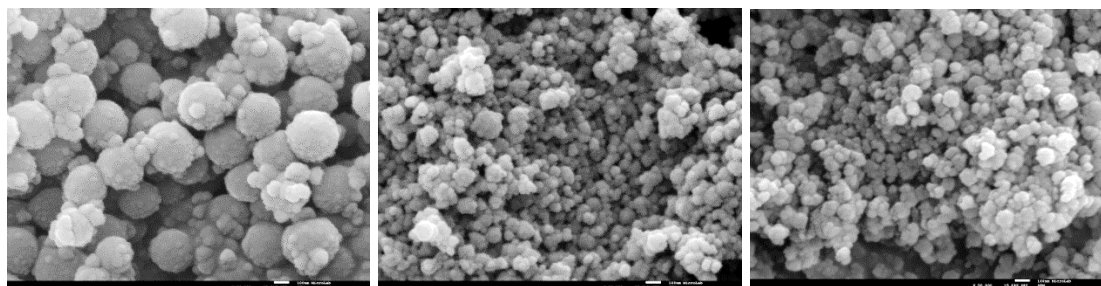


Figure 24 - SEM photomicrographs of SD39, SD40 and SD42 (at the same magnification, scale bar = 100 nm)

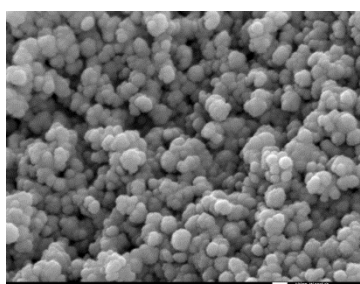


Figure 25 – SEM photomicrograph of SD44 (scale bar = 100 nm)

The process was indeed carried out in a closed system at a controlled temperature, so that the ambient conditions should not affect it, however as the different syntheses were carried out in a span of several months (summer-fall-winter), this fact might have influenced the syntheses results.

A scale-up 2:1 was tried (SD34) but resulted in particles of two different sizes. (Figure 26)

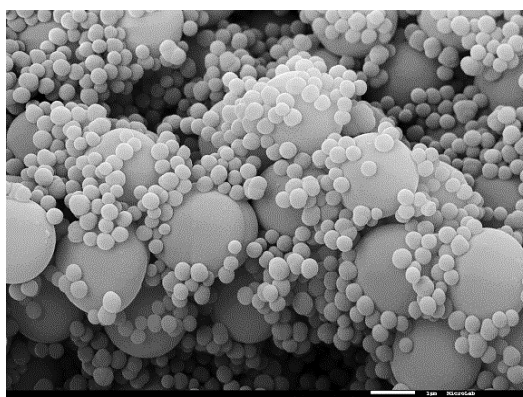


Figure 26 - SEM photomicrograph of SD34 (scale bar = 1 μ m)

The reduction on the concentration of KCl to 92% (SD48) and to 84% (SD46) of its original amount did not result in a visible benefit, in what regards the aggregation issue, when compared with the original KCl concentration (SD44). This also made the centrifugation harder or not possible at all using the same speed. In particular, for SD46 and SD48, it was not possible to centrifuge the reaction product at the current speed, therefore the content was dried in a rotary evaporator with an oil bath at 30°C.

The results are shown in Figure 27, respectively, from left to right, 100%, 92% and 84% concentration of KCl.

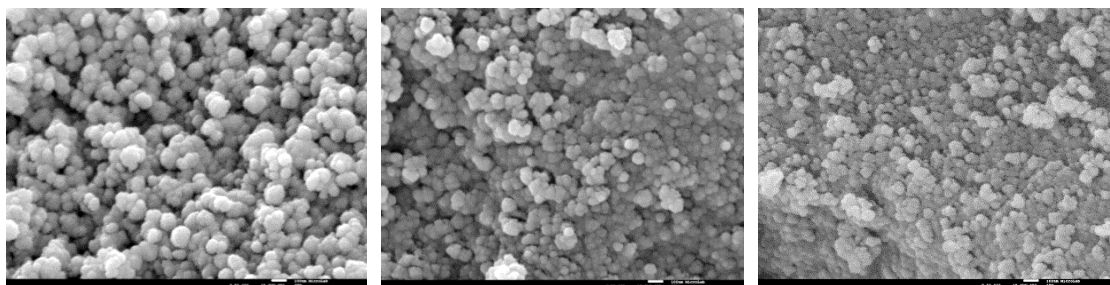


Figure 27 – SEM photomicrographs of SD44 (100% KCl), SD48 (92% KCl) and SD46 (84% KCl) (at the same magnification, scale bar =100 nm)

The SD36 particles showed the best result, as the particles size was smaller, showed a very homogenous size distribution and there was no apparent agglomeration visible. By that reason they were chosen to proceed with the work, i.e. for the emulsion stabilization studies. (Figure 28)

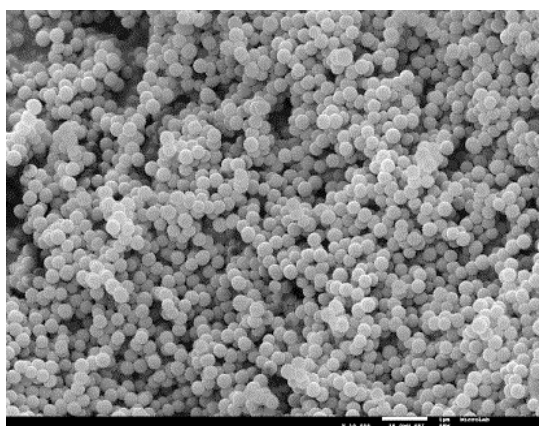


Figure 28 - SEM photomicrograph of SD36 (scale bar = 1 µm)

In what regards the particles chemical structure, FTIR-ATR analyses were carried out. The spectrum of the best particles is shown in Figure 29.

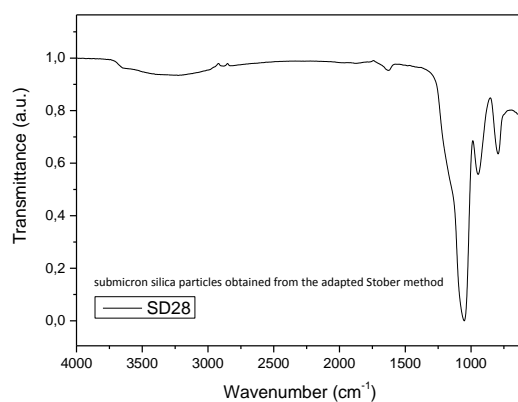


Figure 29 - FTIR spectrum of SD28 particles

The FTIR spectrum (Figure 29) is very similar to the one obtained for the porous microspheres, which is expectable since both are made of silica, however the submicron particles obtained in SD28 do not exhibit any presence of epoxy groups, as expected, since in this synthesis only TEOS was used as Si precursor. So, no peaks at 3050, 1250, 900 and 850 cm⁻¹ are visible in the spectrum.

3.3. Silica commercial particles

The particles received from UBE EXSYMO CO., LTD, were analyzed by SEM and FTIR-ATR.

N2N, according to the producer are non-functionalized inorganic silica particles with 0.2 μm diameter, which can be observed in Figure 30.

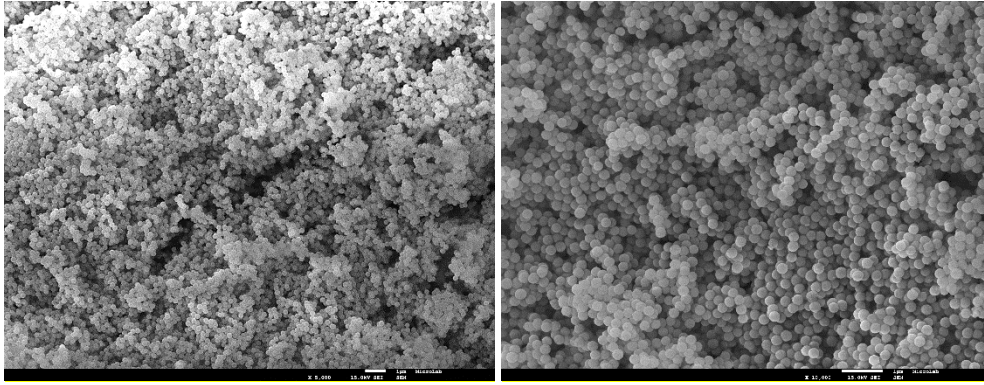


Figure 30 - SEM photomicrographs of N2N (scale bar = 1 μ m)

Particles N3N1 are non-functionalized inorganic silica particles. They can be observed in Figure 31, exhibiting a very uniform size distribution with particles size ca. 1 μ m in diameter, which is in accordance to the information given by the producer/supplier (UBE EXSYMO CO., LTD).

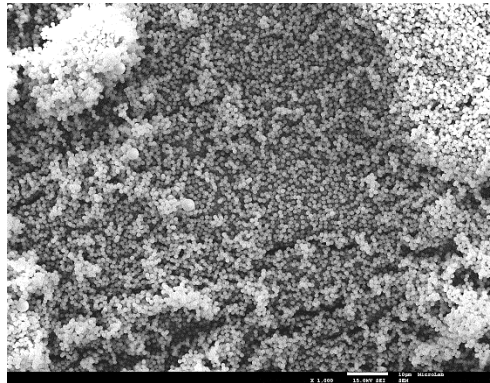


Figure 31 - SEM photomicrograph of N3N1 (scale bar = 10 μ m)

Particles N3N3 are also are non-functionalized inorganic silica particles and are shown (Figure 32) to have 3 μ m of diameter, which is also in accordance to the supplier's information.

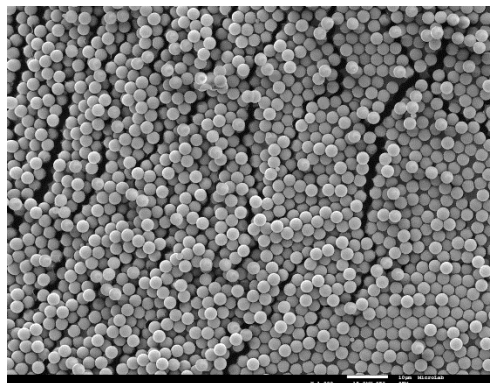


Figure 32 - SEM photomicrograph of N3N3 (scale bar = 10 μ m)

Particles N6N3, on the other hand, are non-functionalized hybrid inorganic-inorganic polyorgano siloxane particles with 3 μm diameter, as observed in Figure 33.

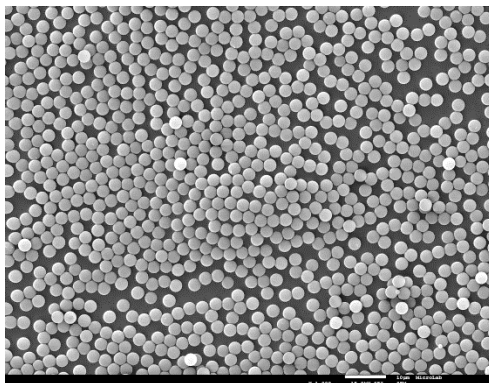


Figure 33 - SEM photomicrograph of N6N3 (scale bar = 10 μm)

3.4. Hydrophobic treatment

The particles used for the hydrophobization treatment, carried out with HDTMS, were SD36 and N2N, and the samples obtained were referred to SD36H and N2NH respectively, throughout this work.

Figure 34 and Figure 35 shows the particles after the hydrophobization process, and Figure 36 and Figure 37 show a comparison of the non-treated and treated particles. A big similarity among those prepared in this work (SD36) and those commercially achieved (N2N) can be depicted.

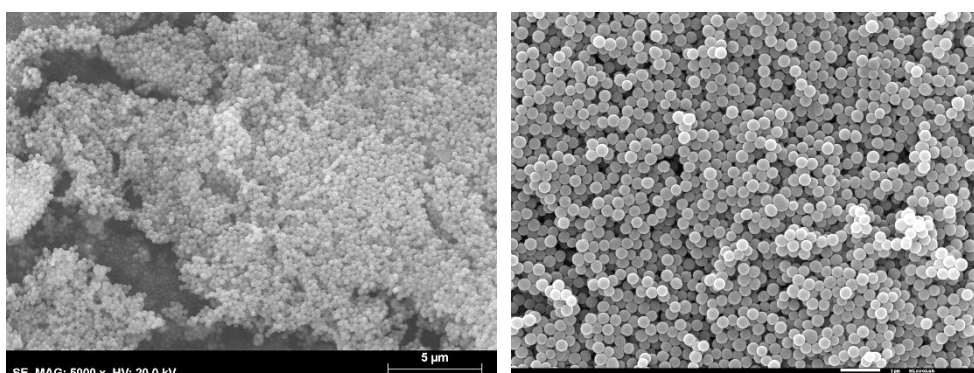


Figure 34 - SEM photomicrographs of SD36H (scale bar = 5 μm at the image of the left and 1 μm at the image of the right)

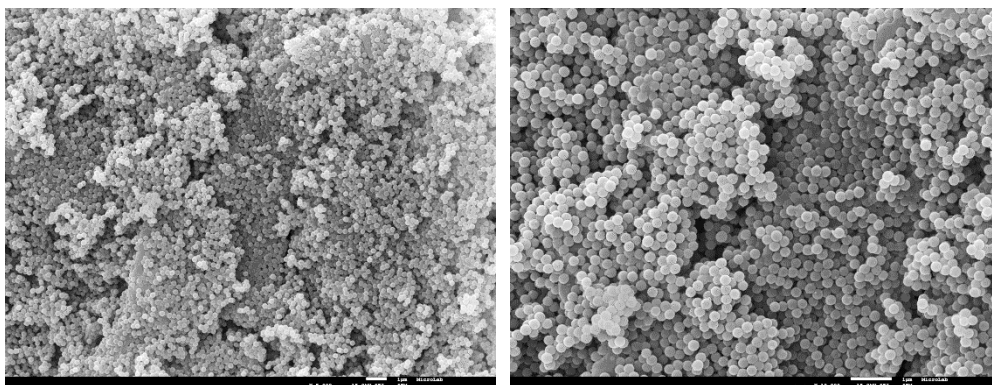


Figure 35 - SEM photomicrographs of N2NH (scale bar = 1 μm)

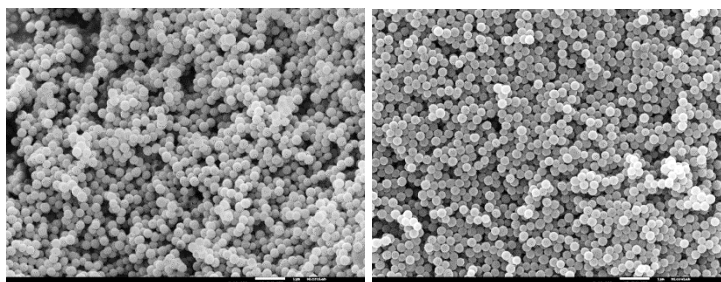


Figure 36 – SEM photomicrographs of SD36 and SD36H (scale bar = 1 μm)

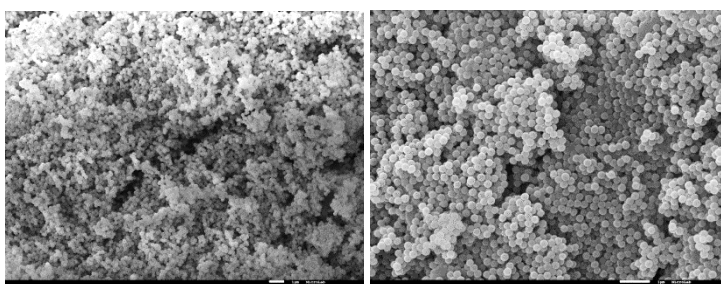


Figure 37 - SEM photomicrographs of N2N and N2NH (scale bar = 1 μm)

The FTIR spectrum (Figure 38) of HDTMS exhibits peaks near 2920 cm^{-1} , near 2850 cm^{-1} and near 1465 cm^{-1} , which are relative to C-H stretching. The peaks near 1190 cm^{-1} and 1065 cm^{-1} are related to Si-O-Si asymmetric vibrations, the peak near 800 cm^{-1} is related to Si-O-Si symmetric stretching vibrations and the small peak near 720 cm^{-1} is relative to the CH_2 rock vibration. The FTIR spectrum of the non-treated SD36 sample shows more OH groups (large band at $\sim 340\text{ cm}^{-1}$ and peak at 1640 cm^{-1}

¹) and Si-OH groups (peak at 950 cm⁻¹) than the non-treated N2N sample, which derives from the different heat treatments that both samples were subject to.

When comparing the spectrum of the SD36 and N2N particles before the treatment (black) and after (red) (Figure 38a and Figure 38b) the treatment, it is possible to see some peaks in common with the HDTMS, which do not appear in the spectrum of the particles before the treatment. Those peaks are at ca. 2920 cm⁻¹, 2850 cm⁻¹ and 1450 cm⁻¹, which are relative to C-H stretching modes and C-CH₂ bonds. These could indicate the presence of HDTMS, since it is the only compound with hydrocarbons in the siloxane network.

Figure 38b indicates not only the presence of the HDTMS, but also that the treatment with HDTMS was more effective on the surface of the particles than in SD36 particles.

Both particles, SD36H and N2NH, were employed in the emulsion stability studies.

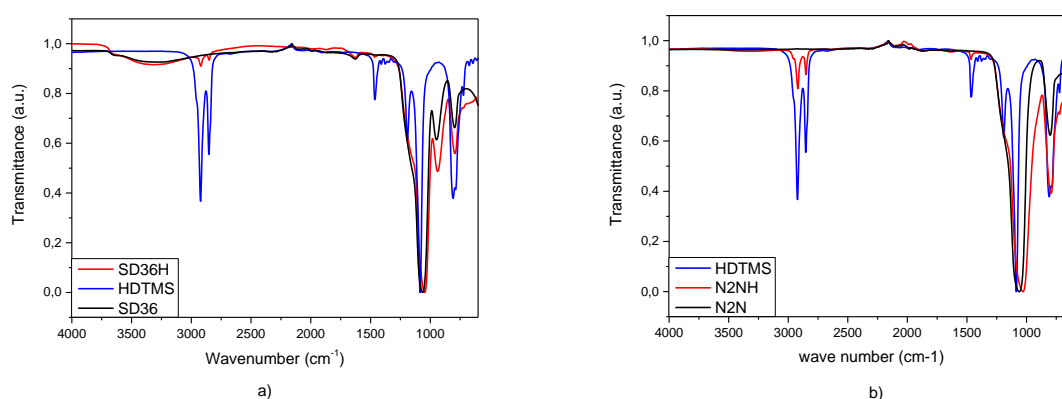


Figure 38 – FTIR spectra of the submicron particles before and after the hydrophobic treatment

PART III – Emulsion stability

3.5. Emulsion stability studies

3.5.1. Effect of the surfactant

The effect of the surfactant type and concentration is studied in this section, in what regards the stability over time of an emulsion prepared with water containing methylene blue (water phase) and decalin (oil phase) at 31/69 v/v%. It should be stressed that, either before the emulsification process, or if there is destabilization of the emulsion with full separation of the water and the oil phases, the appearance of the analysis tube is that shown in Figure 39, with the organic (oil) phase at the top and

blue water, at the bottom. This is due to the fact that a colored dye was added to the water phase and decalin is less dense than water.



Figure 39 – Separation of oil and water phases from an emulsion

Study of SPAN 80

The surfactant typically employed in the synthesis of the porous hybrid microspheres of this work is SPAN 80, added to the oil phase, so that the emulsion stability tests started by assessing the effect of such surfactant. After preparation of the W/O emulsion, at 18000 rpm during minutes, the obtained emulsion was placed in a test tube and it was left to rest during several days. Observation of the emulsions and photographs were taken from time to time and photos of the vessel (test tube) containing the emulsion where 2 g of SPAN 80 were added to decalin, are shown in Figure 40. For this case, it was found that a sedimentation phenomenon occurred liberating an upper oil phase within the first hour after the emulsion preparation. Basically, the oil phase got liberated to the top, while the emulsion went down. It should be noted that the upper oil phase is not totally resolved, i.e. the upper fraction still contains some coalesced colored water droplets, up to at least 4 days, when a top layer of well resolved oil phase starts to appear. The bluish color of the oil phase might result from some migration of methylene blue from the water phase, due probably to some affinity to the OH groups of SPAN 80.

The emulsion did not suffer noticeable change after 8 days.

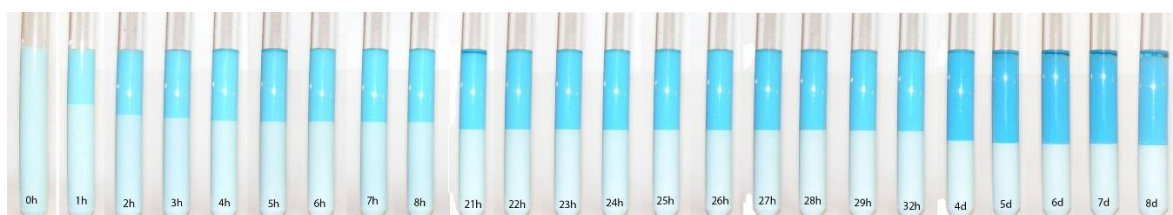


Figure 40 – Evolution of the W/O emulsion using 2g of SPAN 80 added to decalin, from 0 hours to 8 days

Uniformly distributed very small drops are identified from the optical microscopy images at the W/O emulsion (Figure 41) just after being prepared, while significant coalescence of water drops is found to occur within the emulsion fraction in the test tube after 2 weeks.

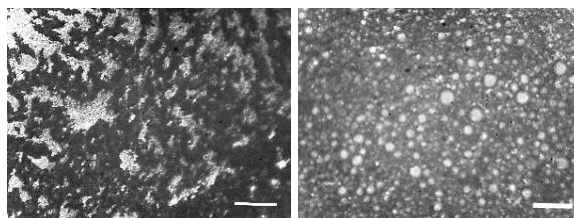


Figure 41 - Optical micrographs of emulsion using 2g of SPAN 80 added to decalin, from 0 hours and at 2 weeks (the white bar represents 100 μm)

The increase in the concentration of SPAN 80 led to an increase of the emulsion stability, as less oil phase got released to the top of the test tube, over the same time period. Figure 42, Figure 44 and Figure 46 show the photographs taken to emulsions prepared with 4, 6 and 8 g of SPAN, added to the oil phase, along the time, which can be compared to the 2 g SPAN 80 results. 6 g of SPAN 80 seem to be the optimum amount of surfactant, since it leads to a slower emulsion destabilization, in the form of sedimentation together with the oil phase release to the top of the test tube.

For these cases, the emulsion samples taken after 2 weeks, observed by optical microscopy, revealed almost no significant changes and therefore the emulsion was considered to remain stable. Figure 43, Figure 45 and Figure 47 are optical micrographs of the emulsion for 0 hours and 2 weeks, and indeed the case where less coalescence of the water droplets occurs is for 4 and 6 g of SPAN 80, which corroborates the results achieved through direct naked eye observation of the test tubes.

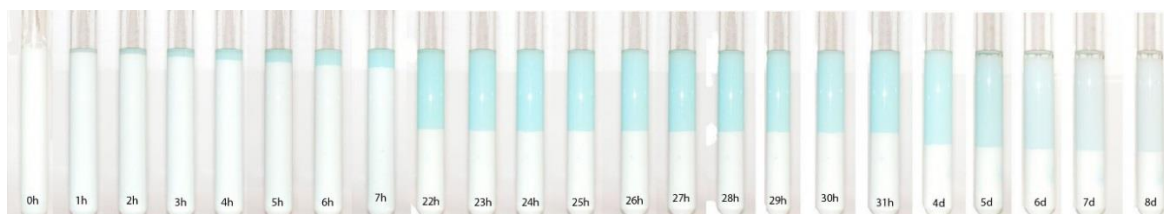


Figure 42 - Evolution of the emulsion using 4g of SPAN 80 from 0 hours to 8 days.

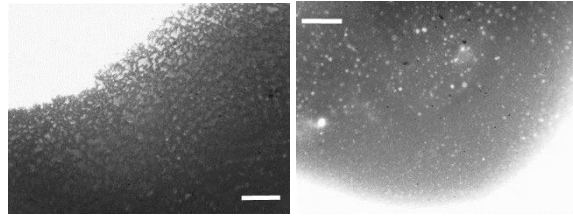


Figure 43 - Optical micrographs of emulsion using 4g of SPAN at 0 hours and at 2 weeks (the white bar represents 100 μ m)

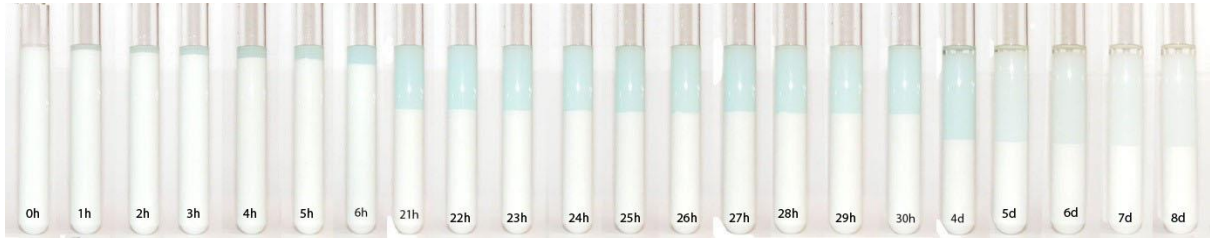


Figure 44 - Evolution of the emulsion using 6g of SPAN 80 from 0 hours to 8 days

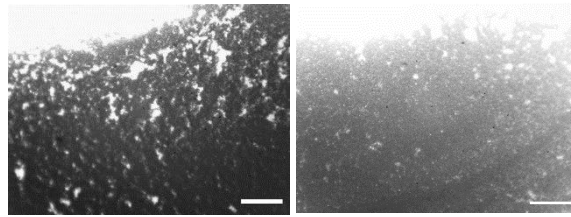


Figure 45 – Optical micrographs of emulsion using 6g at 0 hours and at 2 weeks (the white bar represents 100 μ m)

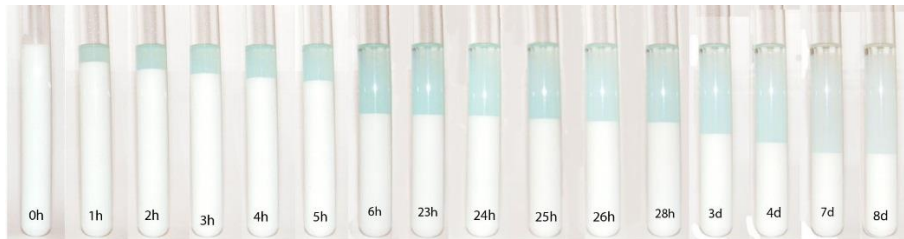


Figure 46 - Evolution of the emulsion using 8g of SPAN 80 from 0 hours to 8 days

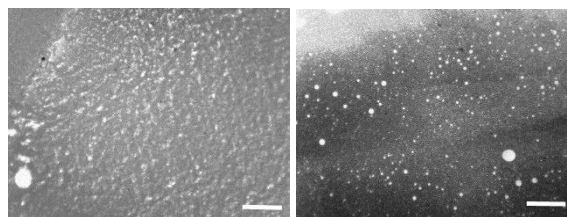


Figure 47 - Optical micrographs of emulsion using 8g at 0 hours and at 2 weeks (the white bar represents 100 μm)

To further study the emulsion stability, the emulsion volume fraction that remains in the test tube over time was compared for the varied concentrations of SPAN 80 (Figure 48). It was concluded that 6 g of SPAN 80 was the optimum amount for this system. It corresponds to the slowest and least intense emulsion destabilization process, within the timeframe studied, which also corroborates the optical microscopy emulsion observation results before described.

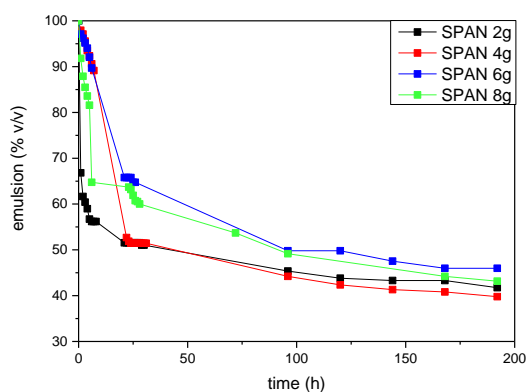


Figure 48 – Plot of the evolution of the emulsion with SPAN 80, i.e. percentage of emulsion remaining along the time, for 2, 4, 6 and 8 g of SPAN 80 added to decalin, the dispersing phase of the emulsion.

Study of Pluronic P123

Pluronic P123 is another type of surfactant that was studied in this thesis. For all Pluronic P123 concentrations tested in this work, the emulsion destabilization phenomenon was based on emulsion sedimentation, as well, together with a very well resolved oil phase liberated to the top of the test tubes. This phenomenon started to occur at a relatively short time and the emulsions did not suffer noticeable change after 3 days. Moreover, the increase in concentration of Pluronic P123 is found to reduce the release of the oil phase over the same time period, as it happened in the study with SPAN 80.

Figure 50, Figure 52, Figure 54, Figure 56, Figure 58 and Figure 60 show the photographs taken to emulsions prepared with 2, 4, 6, 8, 10 and 12 g of Pluronic P123, added to the oil phase, along the time, with the goal of identifying the optimum Pluronic P123 content.

When observing the emulsion part from the test tubes, through optical microscopy, non-uniformly distributed drops were found even for 0 hours, except for 10 and 12 g of Pluronic P123, where a uniform drops size distribution was exhibited for 0 hours and 2 weeks. (Figure 50, Figure 52, Figure 54, Figure 56, Figure 58 and Figure 60)

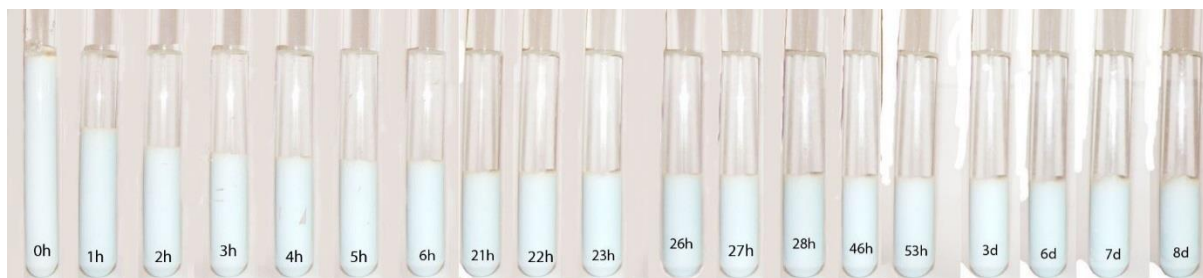


Figure 49 - Evolution of the emulsion using 2g of Pluronic P123 from 0 hours to 8 days

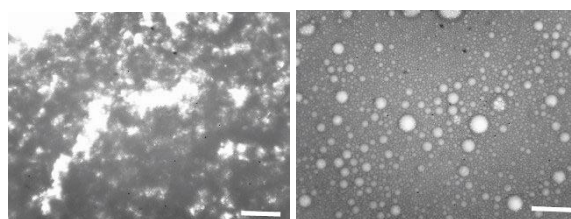


Figure 50 - Optical micrographs of emulsion using 2g of Pluronic P123 at 0h and at 2 weeks (the white bar represents 100 μ m)



Figure 51 - Evolution of the emulsion using 4g of Pluronic P123 from 0 hours to 8 days

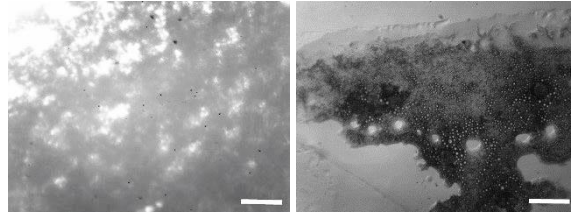


Figure 52 - Optical micrographs of emulsion using 4g of Pluronic P123 at 0 hours and at 2 weeks (the white bar represents 100 μ m)

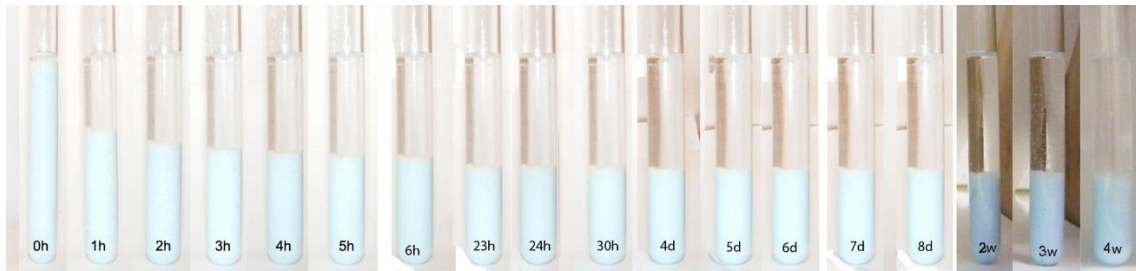


Figure 53 - Evolution of the emulsion using 6g of Pluronic P123 from 0 hours to 8 days

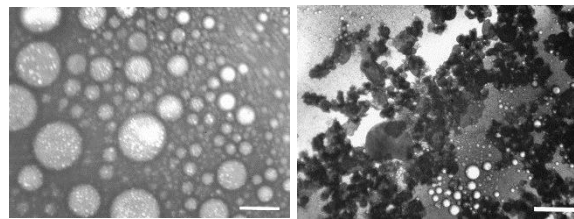


Figure 54 - Optical micrographs of emulsion using 6g of Pluronic P123 0h and at 2 weeks (the white bar represents 100 μ m)



Figure 55 - Evolution of the emulsion using 8g of Pluronic P123 from 0 hours to 8 days

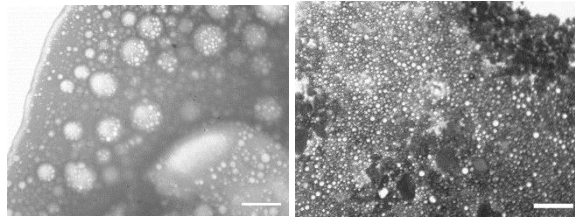


Figure 56 - Optical micrographs of emulsion using 8g of Pluronic at 0 hours and at 2 weeks (the white bar represents 100 μ m)

Two additional studies were conducted by increasing the quantity of Pluronic P123

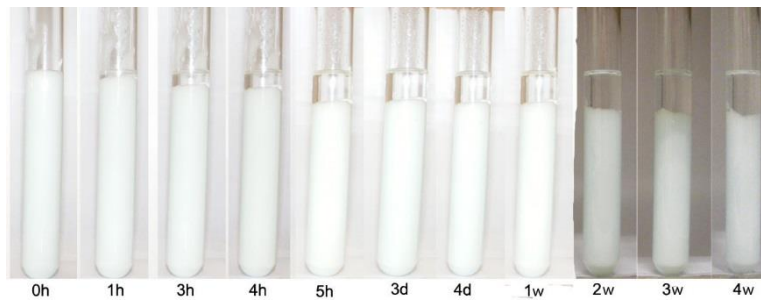


Figure 57 - Evolution of the emulsion using 10g of Pluronic P123 from 0 hours to 4 weeks

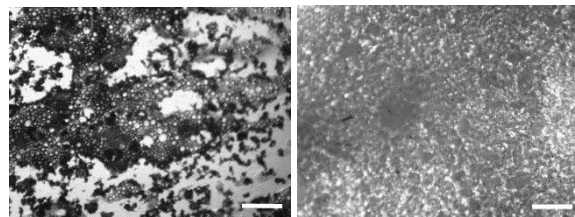


Figure 58 - Optical micrographs of emulsion using 10g of Pluronic P123 at 0 hours and at 2 weeks (the white bar represents 100 μ m)

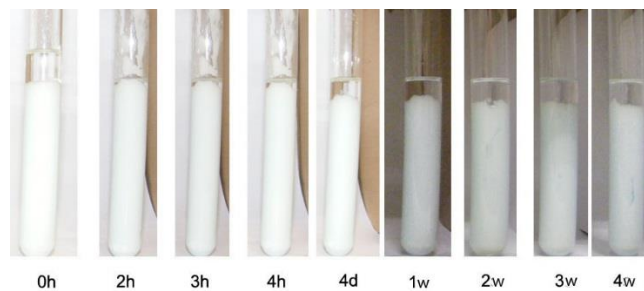


Figure 59 - Evolution of the emulsion using 12g of Pluronic P123 from 0 hours to 4 weeks

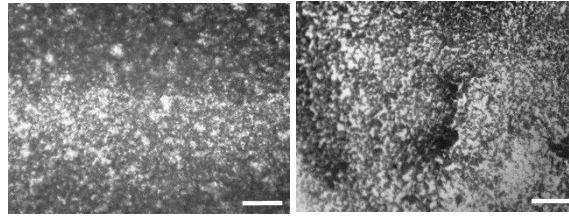


Figure 60 - Optical micrographs of emulsion using 12g of Pluronic P123 at 0 hours and at 2 weeks (the white bar represents 100 μm)

Regarding the evolution of the remaining emulsion over the time, Figure 61, shows a comparison for Pluronic P123 contents from 2 to 12 g. Despite the more resolved oil phase that is liberated to the top of the test tubes and the faster emulsion sedimentation phenomenon, tests with Pluronic P123 show a higher fraction of remaining emulsion (above 65v/v%), especially for 8 g of Pluronic P123 and above, when compared to SPAN 80.

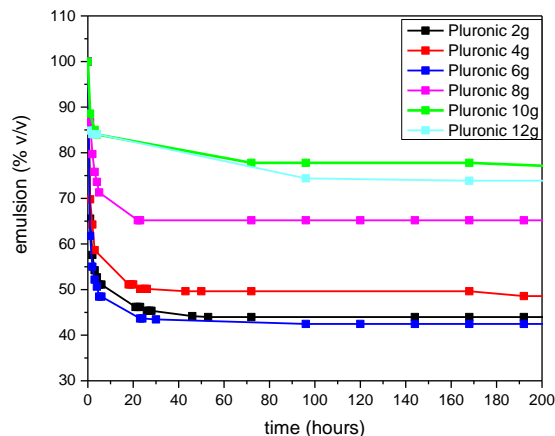


Figure 61 - Plot of the evolution of the emulsion with Pluronic P123.

When comparing the plot results from Figure 61, one can conclude that 10 g of Pluronic P123 (followed by 12 g) is the optimal surfactant amount, which results in less separation and, therefore, in a more stable emulsion.

When comparing both surfactants, at optimum contents, one can conclude that Pluronic P123, at 10g, results in less separation than SPAN 80, at 6 g. Therefore, 10 g of Pluronic P123 might be used as a promising stabilizer for the emulsion employed in the synthesis of the porous microspheres of this work.

The HLB of SPAN 80 is 4.3 while the HLB of Pluronic P123 is 7-12, therefore as indicated before, SPAN 80 should be more suitable for W/O emulsions, such as the one used in this work, and SPAN 80 should have shown better results than Pluronic P123. However, the HLB by itself does not measure the effectivity. [3, 10, 11] To validate these results a test would be done later by using Pluronic instead of SPAN in a sol-gel synthesis. The effectivity of Pluronic P123 will be checked in a real synthesis of the microspheres.

3.5.2. Effect of the particles

The commonly accepted rule is that hydrophilic particles stabilize O/W emulsions, while hydrophobic ones stabilize W/O emulsions [45] however it has been reported that rough particles can be universal Pickering emulsion stabilizers, i.e. they can be used to stabilize both o/w and w/o emulsions [14]. Having this finding into account, particles either hydrophobic or hydrophilic will be placed into the oil phase of the emulsion. All the concentrations are in w/w% of the organic phase.

Study of SD36

By using 0.2% of particles SD36, and no surfactant at all, it was possible to observe emulsion sedimentation phenomenon (Figure 62), together with the releasing of an oil phase at the top. Also, it should be stressed that the quality of the emulsion formed is not good, displaying water droplets with a heterogeneous size distribution and large droplets formed by coalescence (Figure 63). 0.2% of SD36 is definitely not enough to form a stable emulsion, or these particles would be better suited for O/W emulsions.

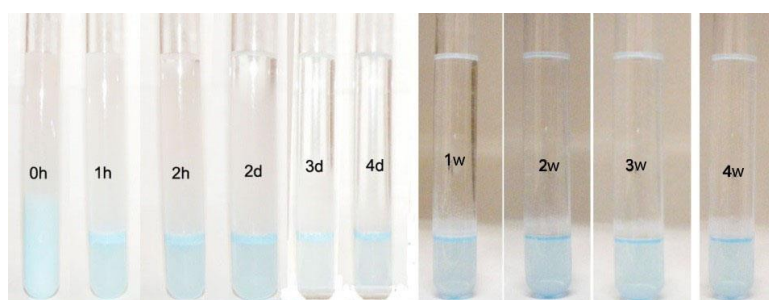


Figure 62 - Evolution of the emulsion using 0.2% of SD36 particles from 0 hours to 4 weeks.

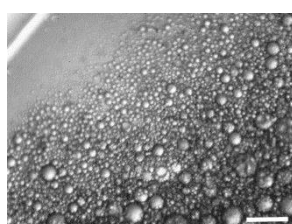


Figure 63 - Optical micrographs of emulsion using 0.2% of SD36 particles at 0 hours (the white bar represents 100 μm)

As SD36 particles concentration increases, more particles are available to cover the surface of the droplets; therefore, the stability would be expected to increase.

Even after increasing the concentration to 2%, even though the release of oil phase is lower, sedimentation still occurred, and the water droplets coalesced progressively as a well resolved water phase appears at the bottom, while some of the particles sedimented at the bottom.

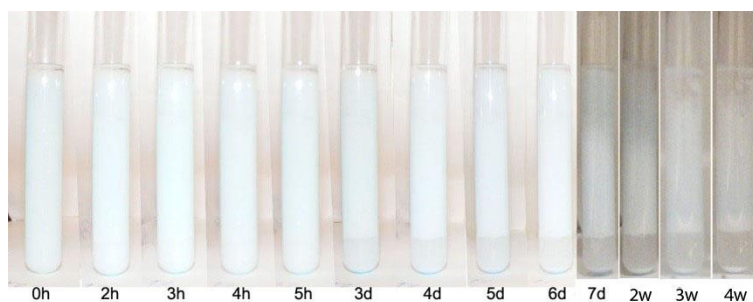


Figure 64 - Evolution of the emulsion using 2% of SD36 particles from 0 hours to 4 weeks.

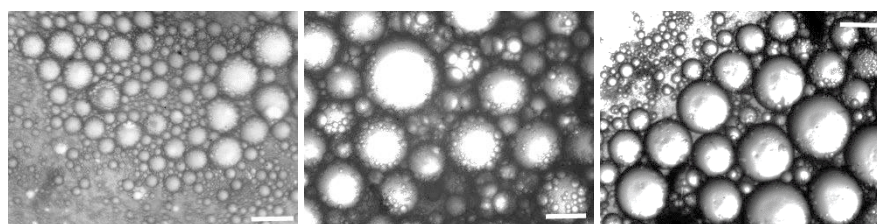


Figure 65 - Optical micrographs of emulsion using 2% of SD36 particles at 0 hours, at 1 week and at 2 weeks (the white bar represents 100 μm)

Study of SD36H

When using the hydrophobized particles, SD36H, emulsion sedimentation was found to occur as well, within the first hour (Figure 66). Some coalescence of the water droplets occurred, since it was visible a white phase, the emulsion, in the middle, and a blue phase, the water phase, at the bottom. Nevertheless, the emulsion remained with almost no changes for the four weeks. The samples of the emulsion taken from the test tube were observed at the optical microscope (Figure 67), confirming the coalescence of the water droplets over time. Due to limitations in the amount of sample SD36H, no further tests were possible using the same particles, and the effect of concentration could not be studied.

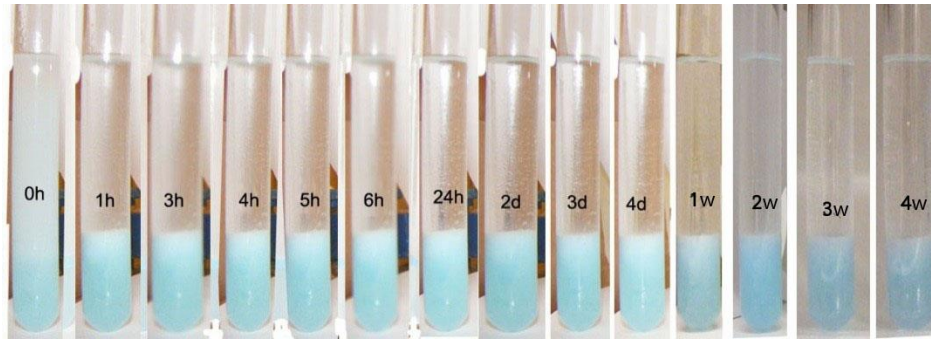


Figure 66 - Evolution of the emulsion using 0.2% of SD36H particles from 0 hours to 4 weeks

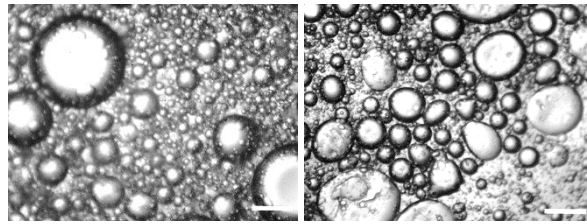


Figure 67 - Optical micrographs of emulsion using 0.2% of SD36H particles at 0 hours and after 4 weeks (the white bar represents 100 μm)

The same method employed for the surfactants study was followed, as the emulsions were compared by measuring the remaining volume fraction over time.

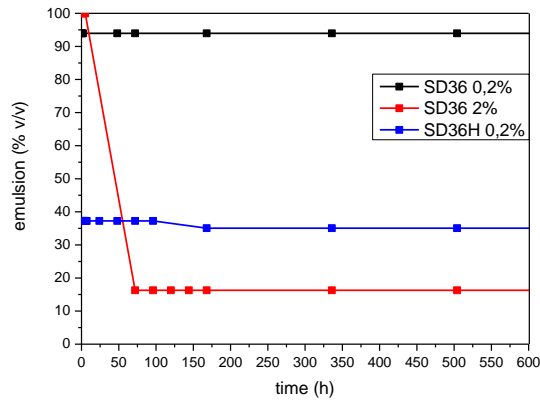


Figure 68 – Plot with the evolution of emulsion with the particles

Since the emulsion in study is W/O type, hydrophobic particles would in theory be more adequate for this type of emulsion and, therefore, lead to smaller droplets and to a better droplets distribution than hydrophilic particles. In fact, in comparison, the SD36H ones provided a more stable emulsion than SD36, despite the tendency for emulsion sedimentation observed. It can be observed that SD36H promote similar results as those in the presence of surfactants.

Study of N3N1

Commercial particles N3N1, of 1 micron in diameter, were tested at varied concentrations in the organic phase, and only when used at contents above 2%, it was possible to form a (very poor) emulsion. Even at 2%, the oil phase was visible at the top and the water phase at the bottom. It was also possible to see the particles (bluish, due to the methylene blue used in the water phase) deposited at the bottom. It is herein suggested that the size of these particles might be too large for this purpose.

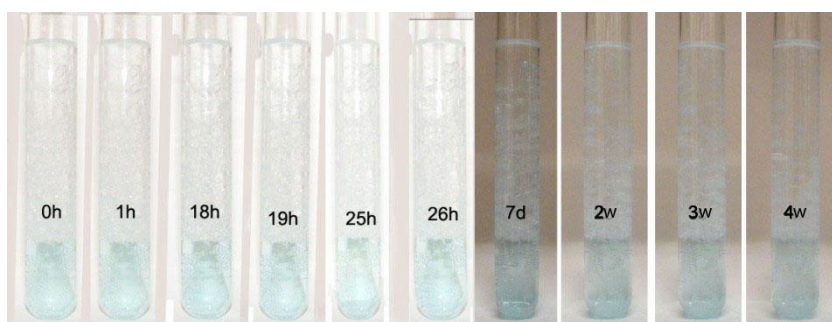


Figure 69 – Evolution of the emulsion using 0.2% of N3N1 particles from 0 hours to 4 weeks

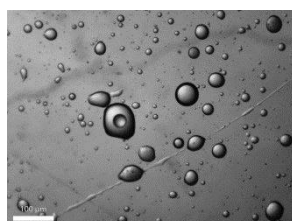


Figure 70 - Optical micrograph of emulsion using 0.2% of N3N1 particles at 0 hours.
(the white bar represents 100 μm)

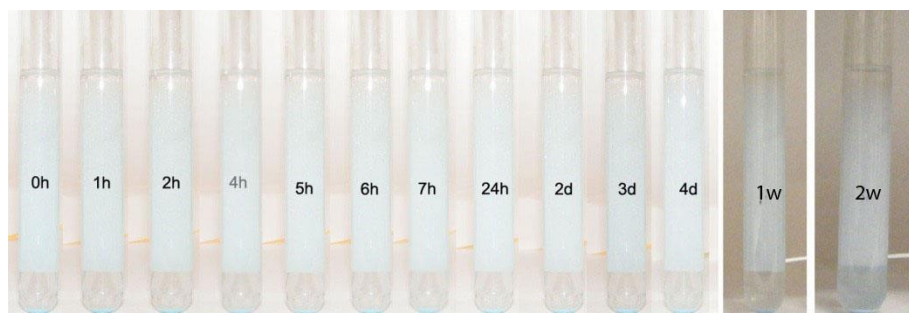


Figure 71 - Evolution of the emulsion using 2% of N3N1 particles from 0 hours to 2 weeks

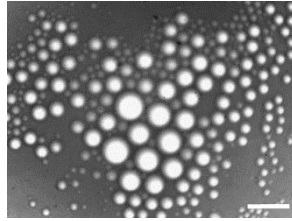


Figure 72 - Optical micrograph of emulsion using 2% of N3N1 particles at 0 hours (the white bar represents 100 μm)

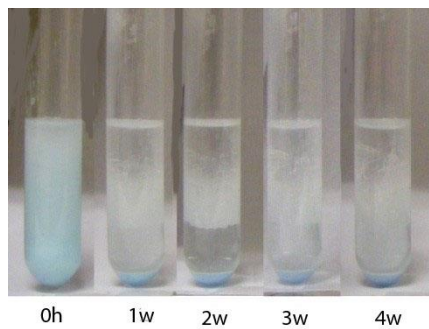


Figure 73 - Evolution of the emulsion using 5.3% of N3N1 particles from 0 hours to 4 weeks

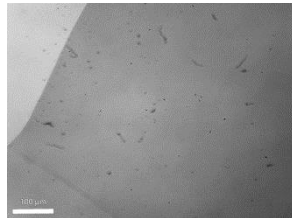


Figure 74 - Optical micrograph of emulsion using 5.3% of N3N1 particles at 0 hours (the white bar represents 100 μm)

Study of N3N3

Commercial particles N3N3 of even larger size than N3N1, with 3 microns in diameter, show similar, or even worst results, than with N3N1, which further suggests that the size of these particles is not adequate for the purpose of this study. For instance, it can be observed in the optical micrographs of Figures 89, 91 and 93, that no emulsion is formed using these particles.

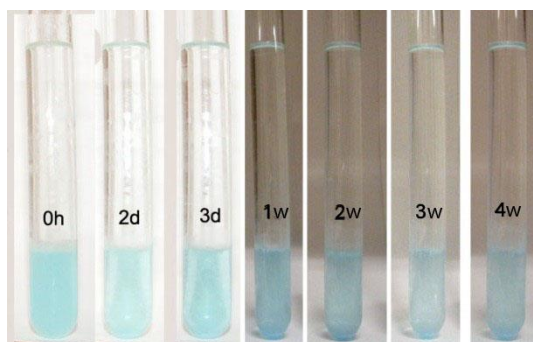


Figure 75 - Evolution of the emulsion using 0.2% of N3N3 particles from 0 hours to 4 weeks

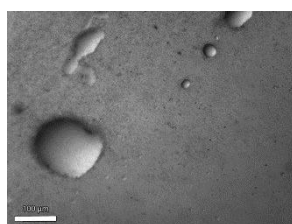


Figure 76 - Optical micrograph of emulsion using 0.2% of N3N3 particles at 0 hours.
(the white bar represents 100 μm)

No emulsion was observed, even at time 0h. Water and oil phases separated immediately after the emulsification process, while the particles remained in water suspension.

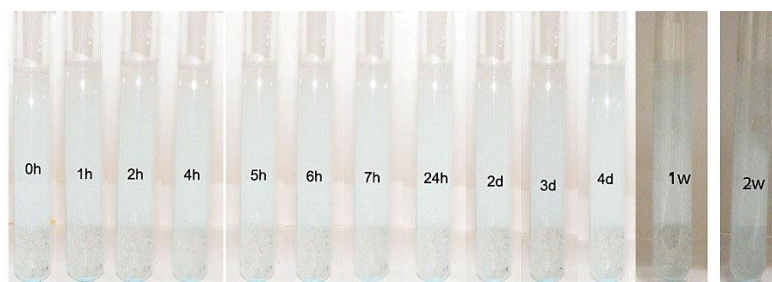


Figure 77 - Evolution of the emulsion using 2% of N3N3 particles from 0 hours to 2 weeks

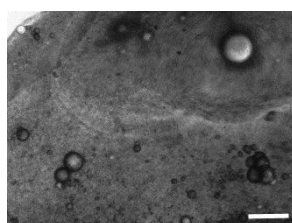


Figure 78 - Optical micrograph of emulsion using 2% of N3N3 particles from 0 hours particles
(the white bar represents 100 μm)

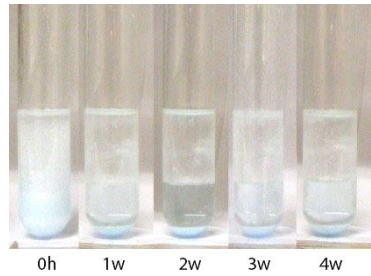


Figure 79 - Evolution of the emulsion using 5.3% of N3N3 particles from 0 hours to 4 weeks

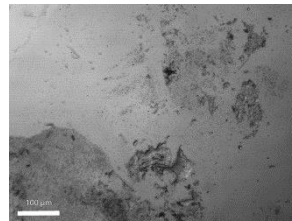


Figure 80 - Optical micrograph of emulsion using 5.3% of N3N3 particles at 0 hours (the white bar represents 100 μm)

Study of N6N3

Commercial particles N6N3 have the same size as N3N3, but do not exhibit the hygroscopic nature of silica, since they were hydrophobized. Due to this fact, they have more compatibility with the O phase. At low concentrations as low as 0.2%, there was no formation of an emulsion (Figure 81 and Figure 82), however at 2% they were able to form an emulsion (Figure 83), however with heterogeneous size distribution (Figure 84), which was immediately followed by creaming, or water droplets coalescence and deposition at the bottom of the test tube. At 5.3% the emulsion formed (not possible to observe at the optical microscope) sedimented at the bottom of the test tube (Figure 85), with the oil phase going upwards.

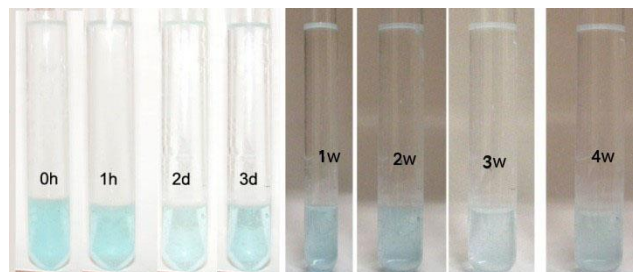


Figure 81 - Evolution of the emulsion using 0.2% of N6N3 particles from 0 hours to 4 weeks.

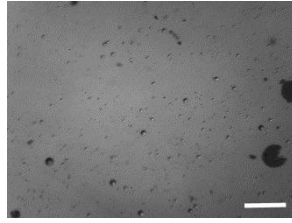


Figure 82 - Optical micrograph of emulsion using 0.2% of N6N3 particles at 0 hours (the white bar represents 100 μ m)



Figure 83 - Evolution of the emulsion using 2% of N6N3 particles from 0 hours to 4 weeks

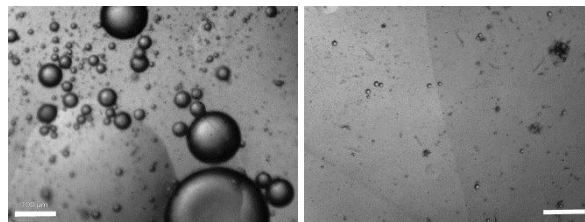


Figure 84 - Optical micrographs of emulsion using 2% of N6N3 particles at 0 hours and at 2 weeks (the white bar represents 100 μ m)

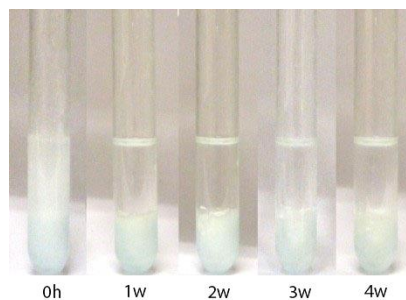


Figure 85 - Evolution of the emulsion using 5.3% of N6N3 particles from 0 hours to 4 weeks

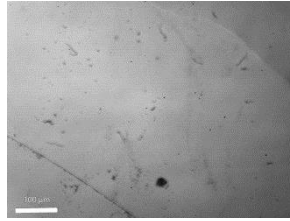


Figure 86 - Optical micrograph of emulsion using 5.3% of N6N3 particles at 0 hours (the white bar represents 100 μm)

The droplets sedimented over time while the particles remained in the water. Flocculation of the particles was observed for the emulsions with 2% and 5.3% of particles.

Smaller size commercial particles of silica composition, N2N, of 200 nm of diameter were tested, i.e. added to the organic phase of the emulsion. A smaller volume of emulsion was prepared in this case, since the amount of particles received from the supplier was not large enough to keep with the same amounts of the previous tests.

Using N2N particles at 2%, there were no apparent changes in the visual aspect of the emulsion until 3 hours, when it was possible to see coalescence, as the water phase was visible at the bottom and, after four days, it was possible to see sedimentation as the oil phase appeared at the top, with the emulsion remaining in the middle. However, as Figure 88 reveals, the droplet size of the emulsion remained quite constant during the first 5 days after emulsion preparation.

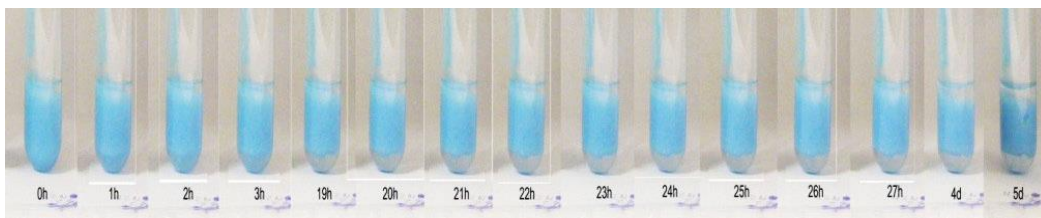


Figure 87 - Evolution of the emulsion using 2% of N2N particles from 0 hours to 5 days

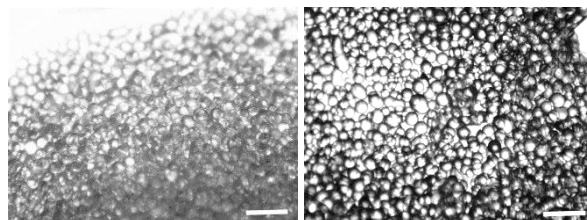


Figure 88 - Optical micrographs of emulsion using 2% of N2N particles at 0 hours and 5 days. (the white bar represents 100 μm)

Study of N2NH

The same particles N2N, but after a hydrophobization treatment, were also tested in terms of their effect in the emulsion stability, at 0.2, 2 and 5.3%. This former concentration was not enough to give a proper emulsion. Droplets were too large, forming, as observed in Figure 89, a white blueish phase, while there was since $t=0$ a dark blue phase composed by the colored water phase at the bottom. With the time, ca. 1 day, the poor emulsion sedimented, with the oil phase migrating to the top of the test tube.

So, it is concluded that when using 0.2% of N2NH particles no emulsification was achieved. Some of the water droplets remained in the oil phase and sediment over time.

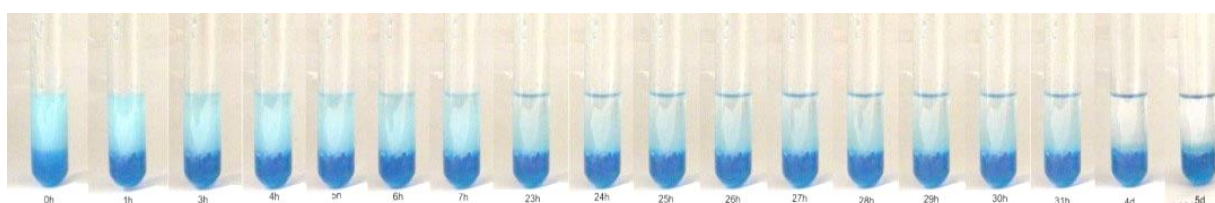


Figure 89 - Evolution of the emulsion using 0.2% of N2NH particles from 0 hours to 5 days

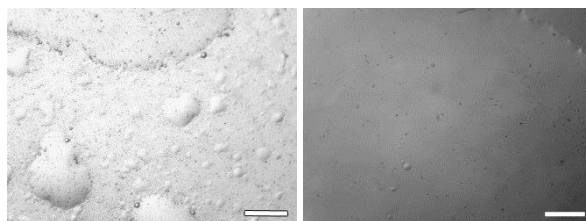


Figure 90 - Optical micrographs of emulsion using 0.2% of N2NH particles from 0 hours and after 1 day (the white bar represents 100 μm)

When the concentration was increased to 2% the emulsification was already possible. Sedimentation occurred as a (well resolved) oil phase got released to the top, but no apparent changes were detected after that, as the emulsion remained stable for the 5 days (Figure 92). This is a similar result to that obtained when using adequate surfactants to this type of emulsion.

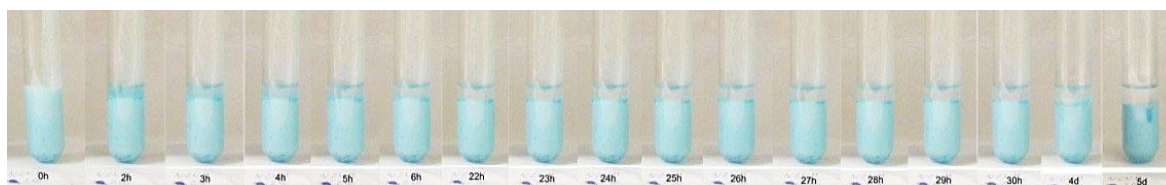


Figure 91 - Evolution of the emulsion using 2% of N2NH particles from 0 hours to 5 days

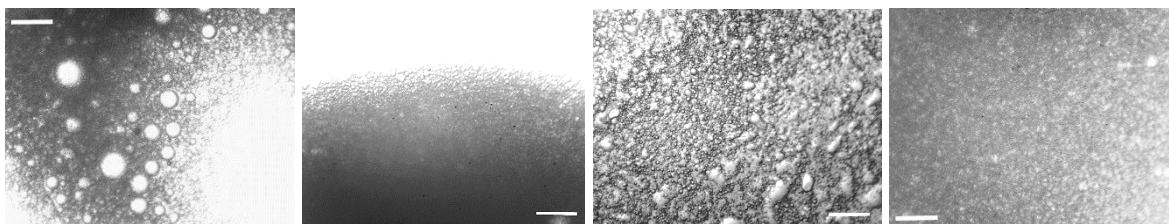


Figure 92 - Optical micrographs of emulsion using 2% of N2NH particles at 0 hours, 1 day, 2 days, 4 days and 5 days. (the white bar represents 100 μm)

When the concentration of N2NH particles was increased to 5.3% once again the sedimentation occurred and no apparent changes were detected after that, as the emulsion remained stable for the 5 days. Very similar results to the ones obtained with 2% of N2NH were achieved, except in the optical micrography that shows an emulsion not so stabilized after 5 days, as in the case of 2% of N2NH.

It could be concluded that 0.2% the particles were insufficient to cover the droplets as no emulsion was formed, however at 2% and 5.3% there were more available particles and therefore could cover the surface of the droplets and prevent their coalescence.

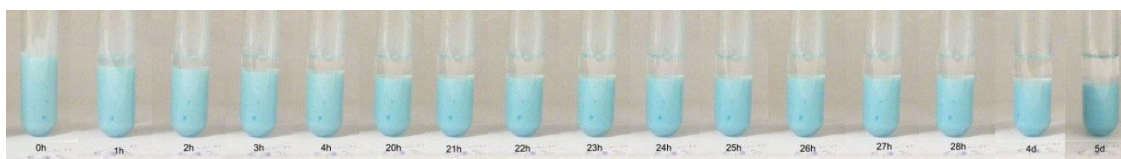


Figure 93 - Evolution of the emulsion using 5.3% of N2NH particles from 0 hours to 5 days

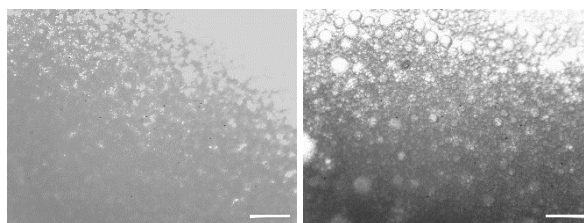


Figure 94 - Optical micrographs of emulsion using 5.3% of N2NH particles at 0 hours and 5 days (the white bar represents 100 μm). The evolution of remaining emulsion volume was analyzed over the time.

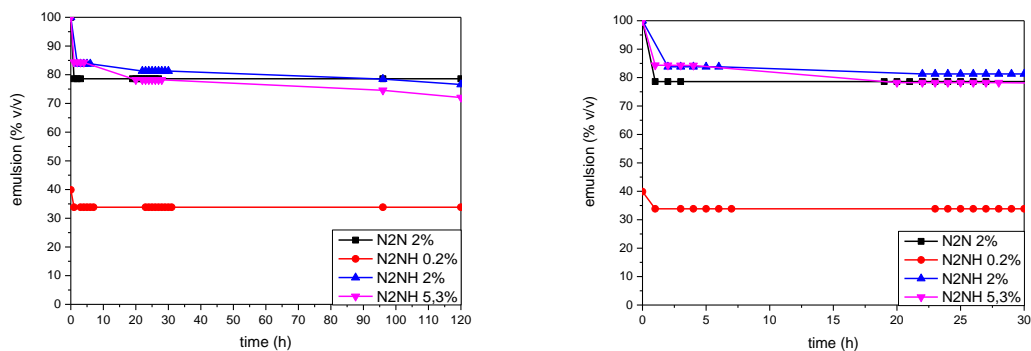


Figure 95 – Plot with the evolution of emulsion with N2N and N2NH particles (with the first 30 h zoomed)

By the plot results the most suitable particle system to use would be the N2NH particles at 2%, since they result in a good compromise between speed of destabilization in the first couple of hours and stability over longer periods of time. They are slightly better than N2NH at 5.3%, in what regards these points.

Comparing with the first set of particles, SD36 and SD36H, N2NH particles were the ones which presented the best performance in what regards the emulsion stabilization of the synthesis of the porous microspheres.


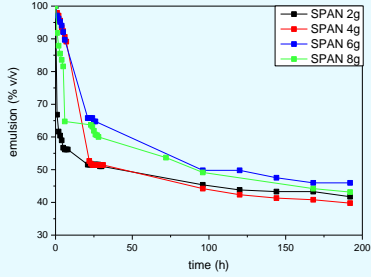

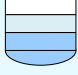

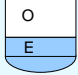
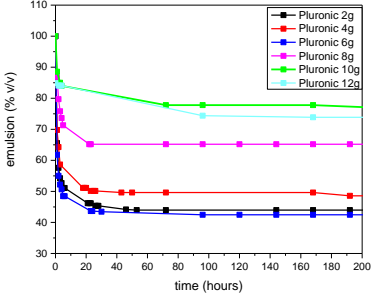


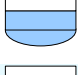
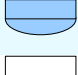
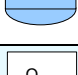
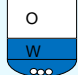
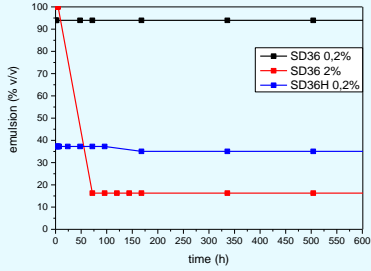


This goes in accordance with the discussion that hydrophobic and smaller particles are more suitable to stabilize W/O emulsions.

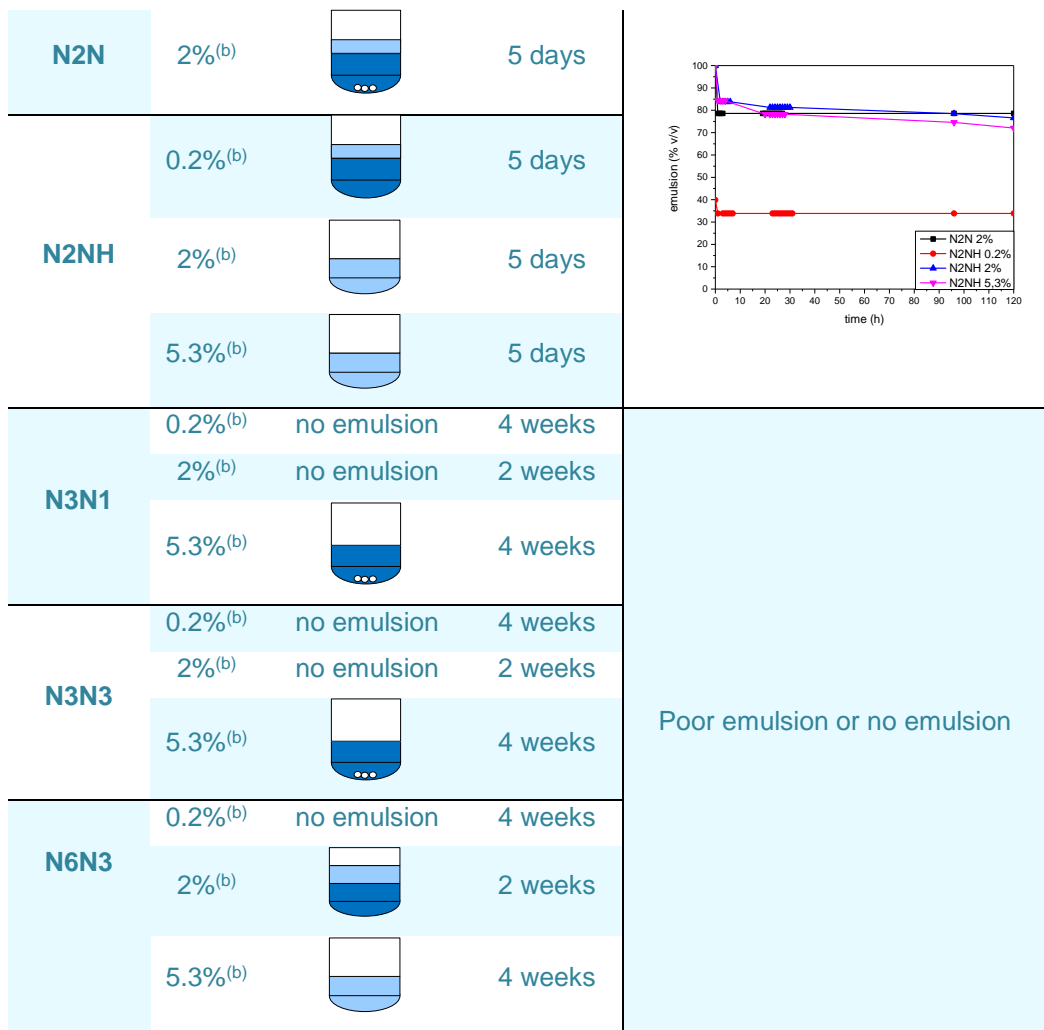
The phase separation phenomenon could be minimized by changing the concentration of the surfactant or the concentration of the particles. Also other parameters outside the framework of this thesis, such as pH could also minimize the phase separation [33]. Moreover, it should be noted that in the targeted synthesis of the porous microspheres, variations in terms of pH and temperature will occur, so this test should also be extended to study the emulsions stability when subjected to such changes. This will be done in a future work.

Finally, since the objective was the development of submicron particles to use as emulsion stabilizers, to confirm if the particles could be used as a replacement of the surfactants, a new sol-gel synthesis, for the production of porous hybrid microspheres, was proposed. In this synthesis the surfactant was replaced by the selected particles, N2NH at 2 wt%, with the purpose of assessing their performance in a real synthesis environment, where no surfactant is used.

Table 10 compiles the result of all the stability studies realized.

Table 10 – Summary and comparison of the emulsion stability study results.

Realized studies	Emulsion schematic ^(a)	Time span of the study	Emulsion %v/v along the time of study
SPAN 80	 2g	2 weeks	
	 4g	2 weeks	
	 6g	2 weeks	
	 8g	2 weeks	
Pluronic P123	 2g	2 weeks	
	 4g	2 weeks	
	 6g	2 weeks	
	 8g	2 weeks	
	 10g	4 weeks	
	 12g	4 weeks	
SD36	 0.2% ^(b)	4 weeks	
	 2% ^(b)	4 weeks	
SD36H	 0.2% ^(b)	4 weeks	



- a) The white color represents the organic phase (O), the light blue the emulsion (E), and the dark blue the water phase (W), PE means poor emulsion, in a flightier blue.
- b) All the percentages are in wt% of the organic phase.

PART IV – Evaluating the stability results on the synthesis process

3.6. New synthesis

The tests with emulsions using 10 g (w/w% organic phase) of Pluronic gave less phase separation instead of using 6 g (w/w% organic phase) of SPAN. Therefore a new synthesis was proposed to evaluate the effect on the microspheres, SD50, using the same sol-gel process method as described before with the exception of replacing SPAN with 10 g (w/w% organic phase) of Pluronic. The particles obtained were characterized under SEM microscopy. The results showed that the particles agglomerate and using 10g of Pluronic did not improve the synthesis like it was expected before, so another synthesis, SD52, was done by reducing the quantity of Pluronic to 8g. (Figure 96).

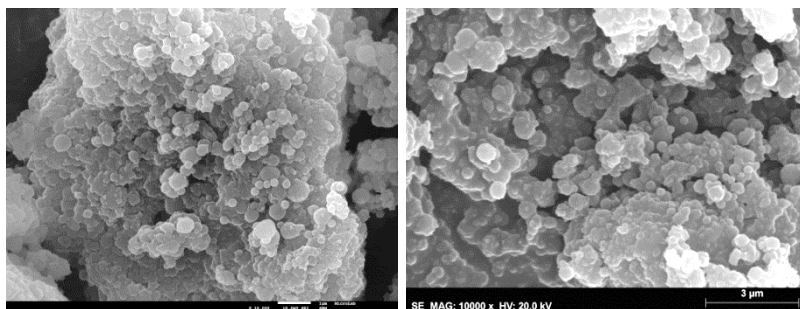


Figure 96 - SEM photomicrographs of SD50 (10g Pluronic P123) and SD52 (8g Pluronic P123) (scale bar = 1 µm)

Even though the quantity of Pluronic was reduced the results showed agglomeration.

Even though the previous stability study showed a better stability when using 10g of Pluronic instead of 6g of SPAN, the results showed that the amount of Pluronic was excessive, even when reduced to 8g, as the particles aggregated. The interface water-oil should be stable, but not to stable to stop the interactions at the interface. Therefore, the synthesis should have been repeated with lower amount.

In the particles study the conclusion was that the hydrophobic modified silica particles increased the stability when in compared with the non-modified ones. The particles chosen were the N2NH of 200 nm in diameter.

A synthesis (SD53) was carried out using the same procedure as indicated before, with the exception of using the particles N2NH at 2wt% (w/w% of the organic phase), instead of SPAN 80. The particles obtained were characterized by SEM. (Figure 97)

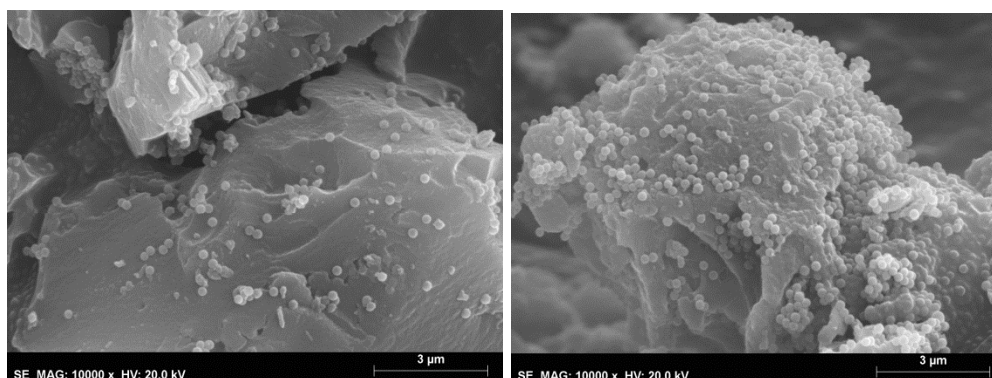


Figure 97 - SEM photomicrographs of SD53 (scale bar = 3 µm)

Even though the previous study showed that the N2NH increase the stability of the emulsions, the synthesis result shows less particles and more agglomeration, due to a probable emulsion destabilization. in comparison to the reference synthesis, using SPAN80.

Observation of the emulsion at the optical microscope was done and photographs were taken during the synthesis. Figure 98 shows the evolution of the emulsion during the synthesis of the microspheres. Stability issues, such as droplet coalescence, are visible at temperatures above 75°C, which is probably responsible for the loose of the spherical morphology of the obtained particles.

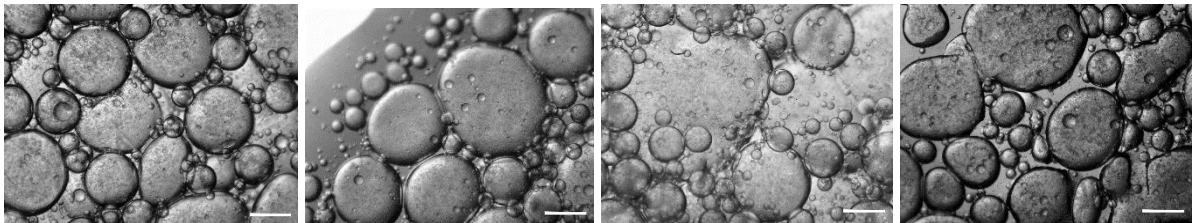


Figure 98 - Optical micrographs of emulsion in the synthesis while using 2% (wt% of the organic phase) of N2NH particles (at 65°C, 70°C, 75°C and 80°C) The white bar represents 100 μm).

Small particles are also observed at the surface of the material obtained in this synthesis, which are the N2NH particles employed. Due to time constraining and also other limitations regarding the amount of N2NH particles, only one trial was done to assess the feasibility of replacing the surfactant SPAN80 by N2NH particles (Pickering emulsion).

Nevertheless, the particles used in the emulsion showed potential to be used as stabilizer in W/O emulsions and therefore could be used in the porous microsphere synthesis process as a replacement of the surfactant, after a more detailed study.

4. Conclusions

This work regards (1st) the optimization of the protocol for the synthesis of porous hybrid microspheres by microemulsion techniques (W/O emulsion) combined with sol-gel processing, (2nd) the synthesis of submicron silica particles and their hydrophobization, to be assessed as Pickering emulsion stabilizers and (3rd) a comprehensive emulsion stability study by means of visual observation and optical microscopy analysis of the emulsion droplets.

Optimum processing parameters for the synthesis of the porous hybrid microspheres, taking into account the best results in terms of particles agglomeration, particle roundness and morphology and desired roughness/porosity, were found to be 18000 rpm of stirring speed of emulsification, 600 rpm of mechanical stirring speed in the reactor and 6 g (w/w% of organic phase) of SPAN 80.

In what regards the submicron silica particles, 300 nm particles in size were obtained using a modified Stöber process, nevertheless it was found to be difficult process to reproduce. In spite of all the efforts, during this work it was not possible to optimize the process in order to control the aggregation, which compromised the achievement of a large enough quantity of particles for the emulsion stability studies.

The hydrophobization of the submicron silica particles prepared in this work, as well as of similar commercial particles was successfully done, using hexadecyltrimethoxysilane, whose long tail of carbons would impart hydrophobicity to the particles' surface. This is important, since hydrophobic particles are more adequate for W/O emulsions. The presence of silane, i.e. the hexadecyl organic functionality at the surface of the particles was confirmed either by FTIR-ATR and SEM. Even though to fully confirm and quantify their hydrophobic character, a measure of the contact angle should have been done.

The surfactant stability studies showed that the use of Pluronic P123 would prevent more oil separation than when using SPAN 80, and hence a more stable emulsion. When using SPAN 80, even though, there was a larger oil separation, the emulsion showed less coalescence, the droplets were of smaller dimension, and the droplet's size distribution seemed more homogeneous.

The particle stability studies (Pickering emulsions) showed that the hydrophobic modified particles, when used at ca. 2-5 wt% of the organic phase, were able to produce more stable emulsions. The best result was achieved for the commercial particles sample HIPRESICA FQ N2N of 0.2 μm in diameter, with the hydrophobic treatment (N2NH). Emulsions with a behavior similar to those obtained with dedicated surfactants were achieved when employing those particles, showing a potential to be used as W/O Pickering emulsion stabilizers in the future.

This work will proceed with the validation of these findings, in what concerns full replacement of SPAN 80 by either Pluronic P123 and by hydrophobized N2N particles in real synthesis experiments of the porous hybrid microspheres. A first trial was already done for both Pluronic P123 and N2NH particles,

but the obtained particles or were not spherical or exhibited tendency to be agglomerated. More optimization trials will need to be done in a near future. Nevertheless, the behavior of the emulsion when using these particles suggests that they could be used to stabilize an emulsion during the sol-gel synthesis, if a more detailed study is performed so the conditions can be optimized.

5. Future work

Some work aspects were not included in this thesis, especially due to lack of time, which are herein suggested:

1. Rheology study of the emulsions
2. Study the effect of other parameters (T, pH) on the stability of the emulsions.
3. Study the effect of the concentration of Pluronic P123 on the porous microspheres synthesis.
4. Optimizing the porous microspheres synthesis parameters while using the hydrophobic particles

6. References

1. Y. Yang *et al.*, An overview of pickering emulsions: Solid-particle materials, classification, morphology, and applications. *Front. Pharmacol.* **8** (2017), doi:10.3389/fphar.2017.00287.
2. C. J. M. Henríquez, W / O Emulsions : Formulation , Characterization and Destabilization Dissertation for the degree of Doctor of Engineering, Brandenburg Technical University, 2009
3. L. L. Schramm, *Emulsions , Foams , and Suspensions*, WILEY-VCH Verlag GmbH & Co. KGaA, Weinheim, 2005.
4. M. V. Loureiro *et al.*, Hybrid custom-tailored sol-gel derived microscaffold for biocides immobilization. *Microporous Mesoporous Mater.* **261**, 252–258 (2018).
5. D. J. McClements, Critical review of techniques and methodologies for characterization of emulsion stability. *Crit. Rev. Food Sci. Nutr.* **47**, 611–649 (2007).
6. Particle sciences drug development services, Emulsion Stability and Testing. *Part. Sci. Drug Dev. Serv.* **2** (2011).
7. A. R. Patel *et al.*, Rheological characterization of gel-in-oil-in-gel type structured emulsions. *Food Hydrocoll.* **46**, 84–92 (2015).
8. A. K. Yegya Raman *et al.*, Emulsion stability of surfactant and solid stabilized water-in-oil emulsions after hydrate formation and dissociation. *Colloids Surfaces A Physicochem. Eng. Asp.* **506**, 607–621 (2016).
9. T. F. Tadros, *Emulsion Formation, Stability, and Rheology*, Wiley VCH Verlag GmbH & Co. KGaA, 2013.
10. ICI Americas Inc, The HLB System. *A time-saving Guid. to Emuls. Sel.* **37**, 1390–3 (1980).
11. V. Madaan, A. chanana, M. K. Kataria, A. Bilandi, Emulsion Technology and Recent Trends in Emulsion Applications. *Int. Res. J. Pharm.* **5**, 533–542 (2014).
12. X. Li *et al.*, Cellulose nanocrystals (CNCs) with different crystalline allomorph for oil in water Pickering emulsions. *Carbohydr. Polym.* **183**, 303–310 (2018).
13. Z. Li *et al.*, Stability mechanism of O/W Pickering emulsions stabilized with regenerated cellulose. *Carbohydr. Polym.* **181**, 224–233 (2018).
14. M. Zanini *et al.*, Universal emulsion stabilization from the arrested adsorption of rough particles at liquid-liquid interfaces. *Nat. Commun.* **8**, 1–9 (2017).

15. S. U. Pickering, *Emulsions*, (1907).
16. B. P. Binks, S. O. Lumsdon, Influence of particle wettability on the type and stability of surfactant-free emulsions. *Langmuir*. **16**, 8622–8631 (2000).
17. Z. Wang, Y. Wang, Tuning Amphiphilicity of Particles for Controllable Pickering Emulsion. *Materials (Basel)*. **9** (2016), doi:10.3390/ma9110903.
18. J. Frelichowska, M. A. Bolzinger, Y. Chevalier, Pickering emulsions with bare silica. *Colloids Surfaces A Physicochem. Eng. Asp.* **343**, 70–74 (2009).
19. B. P. Binks, S. O. Lumsdon, Transitional phase inversion of solid-stabilized emulsions using particle mixtures. *Langmuir*. **16**, 3748–3756 (2000).
20. I. E. Salama, A. Paul, Emulsions of fluorinated oils stabilised by fluorinated silica nanoparticles. *Colloids Surfaces A Physicochem. Eng. Asp.* **494**, 125–138 (2016).
21. L. Zheng *et al.*, New pickering emulsions stabilized by silica nanowires. *Colloids Surfaces A Physicochem. Eng. Asp.* **482**, 639–646 (2015).
22. B. P. Binks, S. O. Olusanya, Pickering emulsions stabilized by coloured organic pigment particles. *Chem. Sci.* **8**, 708–723 (2016).
23. X. Lu, J. Xiao, Q. Huang, Pickering emulsions stabilized by media-milled starch particles. *Food Res. Int.* **105**, 140–149 (2018).
24. B. Pang, H. Liu, P. Liu, X. Peng, K. Zhang, Water-in-oil Pickering emulsions stabilized by stearylated microcrystalline cellulose. *J. Colloid Interface Sci.* **513**, 629–637 (2018).
25. E. J. Leal-Castañeda *et al.*, Pickering emulsions stabilized with native and lauroylated amaranth starch. *Food Hydrocoll.* **80**, 177–185 (2018).
26. S. K. Ghosh, *Functional Coatings by Polymer Microencapsulation*, WILEY-VCH Verlag GmbH & Co. KGaA, Weinheim, 2006.
27. C. J. Brinker, *SOL-GEL SCIENCE The Physics and Chemistry of Sol-Gel Processing*, Academic Press, 1990.
28. Q. Chen *et al.*, Effect of synthesis time on morphology of hollow porous silica microspheres. *Medziagotyra*. **18**, 66–71 (2012).
29. I. Kaltzakorta, E. Erkizia, Study on the effect of sol-gel parameters on the size and morphology of silica microcapsules containing different organic compounds. *Phys. Status Solidi*. **7**, 2697–2700 (2010).

30. R. Ciriminna, M. Sciortino, G. Alonzo, A. de Schrijver, M. Pagliaro, From molecules to systems: sol-gel microencapsulation in silica-based materials, *Chem. Rev.* **111** (2), 765-89 (2011)
31. A. F. S. E. Hüsing, Hierarchical Organization in Monolithic Sol–Gel Materials. *Handb. Sol-Gel Sci. Technol.*, 1–49 (2016).
32. E. B. W. Stober, A. Fink, Controlled Growth of Monodisperse Silica Spheres in the Micron Size Range 1. *Journal Colloid Interface Sci.* **26**, 62–69 (1968).
33. K. S. Rao, K. El-Hami, T. Kodaki, K. Matsushige, K. Makino, A novel method for synthesis of silica nanoparticles. *J. Colloid Interface Sci.* **289**, 125–131 (2005).
34. B. P. Binks, R. Murakami, S. P. Armes, S. Fujii, Effects of pH and Salt Concentration on Oil-in-Water Emulsions Stabilized Solely by(...), *Langmuir*, **22**, 5, 2050-2057 (2006).
35. A. Santiago, A. González, J. J. Iruin, M. J. Fernández-Berridi, L. Irusta, Preparation of superhydrophobic silica nanoparticles by microwave assisted sol-gel process. *J. Sol-Gel Sci. Technol.* **61**, 8–13 (2012).
36. D. Zang, M. Zhang, F. Liu, C. Wang, Superhydrophobic/superoleophilic corn straw fibers as effective oil sorbents for the recovery of spilled oil. *J. Chem. Technol. Biotechnol.* **91**, 2449–2456 (2016).
37. H. Gu, Q. Zhang, J. Gu, N. Li, J. Xiong, Facile preparation of superhydrophobic silica nanoparticles by hydrothermal-assisted sol–gel process and effects of hydrothermal time on surface modification. *J. Sol-Gel Sci. Technol.* **87**, 478–485 (2018).
38. L. Xu, L. Wang, Y. Shen, Y. Ding, Z. Cai, Preparation of hexadecyltrimethoxysilane-modified silica nanocomposite hydrosol and superhydrophobic cotton coating. *Fibers Polym.* **16**, 1082–1091 (2015).
39. W. A. Daoud, J. H. Xin, X. Tao, Superhydrophobic silica nanocomposite coating by a low-temperature process. *J. Am. Ceram. Soc.* **87**, 1782–1784 (2004).
40. X. Huang, X. Fang, Z. Lu, S. Chen, Reinforcement of polysiloxane with superhydrophobic nanosilica. *J. Mater. Sci.* **44**, 4522–4530 (2009).
41. N. D. Hegde, A. Venkateswara Rao, Organic modification of TEOS based silica aerogels using hexadecyltrimethoxysilane as a hydrophobic reagent. *Appl. Surf. Sci.* **253**, 1566–1572 (2006).
42. A. Pourjavadi, H. Esmaili, M. Nazari, Facile fabrication of superhydrophobic nanocomposite coating using modified silica nanoparticles and non-fluorinated acrylic copolymer. *Polym. Bull.* **75**, 4641–4655 (2018).

43. S. Zhang, G. L. Li, H. L. Cong, B. Yu, X. Y. Gai, Size control of monodisperse silica particles by modified Stöber method. *Integr. Ferroelectr.* **178**, 52–57 (2017).
44. J. U. N. Matsuoka, M. Numaguchi, S. Yoshida, N. Soga, Heat of Reaction of the Hydrolysis-Polymerization Process of Tetraethyl Orthosilicate in Acidic Condition. *J. Sol-Gel Sci. Technol.* **19**, 661–664 (2000).
45. B. Smith, *Infrared Spectral Interpretation: A Systematic Approach*, London, CRC Press, 1999).
46. Bennard P. Binks; Tommy S. Horosov, *Colloidal Particles at Liquid Interfaces* (Cambridge University Press, Cambridge, 2009).